

Phase relations of hydrous mantle subducting to 300 km

PETER ULMER and VOLKMAR TROMMSDORFF

Institute for Mineralogy and Petrography, ETH-Zurich, ETH-Zentrum, CH-8092 Zurich, Switzerland

Abstract—Water has profound effects on fundamental geologic processes in the earth's mantle such as magma generation, metasomatism, viscosity and density of solid and molten rocks. In this chapter the significance of hydrated subducting mantle is evaluated as an H₂O-carrier, transporting water from the earth's surface deep into the subduction zone where it is released to the overlying mantle wedge through the breakdown of hydrous phases. The capacity to store and transport H₂O in the hydrated part of the subducted mantle is controlled by the pressure-temperature stability of hydrous phase assemblages in peridotitic bulk compositions. Experimental results, field-based studies and theoretical calculations identify the serpentine mineral antigorite as the most important and chlorite as a subordinate H₂O-carrier to a depth ≤ 200 km. At greater depth, the DHMS (dense hydrous magnesium silicate) phase A (coexisting with enstatite) is the prominent H₂O-reservoir along a cold subduction path to a depth approaching 300 km where phase E, another DHMS phase, is stabilized. Talc is only important at shallow depth (≤ 60 km) and has a limited capacity to carry H₂O into subduction zones due to its low modal abundance in peridotitic compositions. Amphiboles persist to higher temperatures where serpentines are no longer stable, but are restricted to depths of less than 80 km. Titanian-hydroxyl-humite minerals have wide stability fields, they are minor in quantity, but may serve as a sink for high field strength elements. Phase relations above 10 GPa (corresponding to depths of 300 km) are not covered in this section; they are the subject of chapter 16 by D. FROST.

INTRODUCTION

Potential role of ultramafic compositions for the deep subduction of H₂O

The subduction of oceanic lithosphere, composed of peridotitic mantle, plutonic cumulates and gabbros, basaltic volcanics and pelitic to carbonate sediments, is the most efficient material recycling process in the earth's upper mantle and transition zone. In this chapter one particular aspect of material transport is evaluated, the subduction and release of H₂O in the ultramafic peridotitic part of the subducted oceanic lithosphere. In the past, hydrated basaltic compositions represented by gabbroic and volcanic rocks and pelitic compositions corresponding to ocean floor sediments have been favoured as potential H₂O-reservoirs in the subducted oceanic lithosphere. Amphibole was thought to represent the dominant H₂O-carrier (e.g., TATSUMI, 1986; DAVIES and STEVENSON, 1992) in basaltic compositions. Phengitic white mica (e.g., MASSONE and SCHREYER, 1989; SCHMIDT, 1996; DOMANIK and HOLLOWAY 1996) was proposed as an additional H₂O repository in the pelitic metasediments. The ultramafic, crustal cumulates and the upper part of the harzburgitic to lherzolitic mantle underlying the oceanic crust were not considered to be of particular importance as a potential H₂O-reservoir. Consequently, the stability of hydrous minerals in ultramafic compositions was only occasionally the subject of intense experimental research.

Several observations led to a partial change of this view focused towards the basaltic and pelitic com-

positions as the sole H₂O-reservoirs in subducted oceanic lithosphere:

(1) The intensity of hydration of the oceanic lithosphere was strongly underestimated, only the top 1–2 km were considered, neglecting the widespread occurrence of strongly serpentinized ultramafics in ophiolites and on the ocean floor. Recent investigations of ultramafic rocks occurring in ophiolites revealed that intensive serpentinization occurred during metamorphism in the oceanic environment (for a comprehensive review see O'HANLEY, 1996). The oceanic drilling projects confirmed the presence of intensively serpentinized peridotites in a variety of tectonic settings: In the vicinity of both fast (e.g., East Pacific Rise, FRUEH-GREEN *et al.*, 1996) and slow (e.g., Southwest Indian Ridge, MULLER *et al.*, 1997) spreading ridges, as well as along passive continental margins (e.g., Galicia margin, BOILLOT *et al.*, 1988). Several studies explicitly imply that the oceanic MOHO indeed corresponds to the limit between serpentinized and non-serpentinized peridotites, and hence represents a serpentinization front (e.g., COULTON *et al.*, 1995; MULLER *et al.*, 1997).

(2) The role of amphibole as the dominant H₂O-carrier in subduction became debatable when experimental studies revealed that other hydrous silicate phases are stable to considerable pressures and temperatures in the basaltic and ultramafic compositions. A number of studies demonstrated that lawsonite, zoisite, chlorite, and Mg-chloritoid (PAWLEY, 1994; SCHMIDT and POLI, 1994; POLI and SCHMIDT, 1995) are stable to higher pressures than amphibole in basaltic

compositions. The high pressure stability of serpentine group minerals was the subject of several studies in the last 30 years: PISTORIUS (1963), KITAHARA *et al.* (1966), YAMAMOTO and AKIMOTO (1977), KHODYREV and AGOSHKOV (1986), and TATSUMI (1986) investigated the high pressure stability of either synthetic or natural chrysotile or lizardite. Their conclusions regarding the importance of serpentine as a potential H₂O-carrier in subduction zones varied from unimportant to considerably important. The major shortcoming of serpentine was the limited temperature stability, not exceeding 500°C at 4–5 GPa. More recently, ULMER and TROMMSDORFF (1995), WUNDER and SCHREYER (1997) and BOSE and NAVROTSKY (1998) have studied the high-pressure stability of natural and synthetic antigorite, the serpentine mineral observed in high temperature metamorphic terrains. The thermal stability of antigorite is considerably higher than that of chrysotile or lizardite, 650–700°C at 2–4 GPa, increasing the probability of its survival during cold subduction and increasing its potential as an H₂O-carrier to depth. Chlorite forms an additional hydrate phase in ultramafic compositions. The limited data available on the high-pressure behavior of chlorite (FOCKENBERG, 1995) indicate that it is stable to more than 5 GPa at temperatures as high as 700 to 900°C. The classical study of YAMAMOTO and AKIMOTO (1977) revealed that a large number of additional, so called dense hydrous magnesium silicate (DHMS) phases, can be stabilized beyond the stability region of serpentine at temperatures up to 1000°C. The importance of these phases has partly been questioned by LUTH (1995). The complex nature of phase relations of dense hydrous magnesium silicates, also called alphabet phases, will be discussed in paragraph 4 and is the subject of chapter 16 by D. FROST.

(3) The thermal structure of the subducted oceanic lithosphere was poorly known. Thermo-mechanical modeling inferred relatively hot temperatures of 1000°C at the slab-mantle interface at 120 km depth (*e.g.*, HONDA and UYEDA, 1983). Therefore, only hydrate minerals with a high temperature stability such as amphibole could be stable to 100 km. TATSUMI (1986), for example, emphasizes that the slab is essentially anhydrous beneath a volcanic front, *i.e.* at approximately 150–200 km.

The inference from seismic studies and the ocean drilling programs that deeply serpentinized oceanic mantle exists several km below the ocean floor opens the possibility of very cold subduction paths for hydrated oceanic mantle. Evidence for such cold subducted hydrated oceanic lithosphere is present in several high pressure/low temperature eclogite ter-

rains in the Alps and elsewhere (*e.g.*, Liguria, SCAMBELLURI *et al.*, 1995; Zermatt-Saas Zone, BARNICOAT and FRY, 1986; Certo de Almiraz, Sierra Nevada, Spain; TROMMSDORFF *et al.*, 1998) which all include serpentinites associated with basaltic eclogites. Thermo-mechanical modeling (PEACOCK, 1990; DAVIES and STEVENSON, 1992; FURUKAWA, 1993) indicates considerably cooler environments in the interior of slabs than at the slab-mantle interface. Temperatures of 500°C at 200 km depth might well be realized within subducting slabs. The implication that the top part of the ultramafic rocks of the subducted oceanic lithosphere may not only be hydrated but also cold during subduction demands a reevaluation of the stability of hydrous minerals in such compositions and their potential role as H₂O-carriers to great depth.

Importance of H₂O for 'convergent plate boundary processes'

The importance of H₂O for processes occurring in and above the subducted oceanic lithosphere has been addressed by numerous studies over the last 70 years. BOWEN (1928) realized the importance of H₂O for lowering the melting points of silicate materials and for decreasing the viscosity of liquid silicates. Since then many studies have substantiated that H₂O is required for the generation of calc-alkaline island arc magmas in supra-subduction settings (*e.g.*, WYLLIE, 1971; KUSHIRO, 1972, 1987, 1990; GREEN, 1973; GREEN, 1980; RINGWOOD, 1974; MYSEN and BOETTCHER, 1975; TATSUMI, 1986; TATSUMI *et al.*, 1983). H₂O considerably lowers the melting point of peridotitic mantle and enhances the amount of partial melting. Given that the ambient temperature of the mantle wedge above the subducting slab is not higher than the average current mantle adiabat (ACMA), only the depression of the melting point by addition of H₂O released from the subducting slab can lead to generation of basaltic/picritic magmas in the mantle wedge. It is widely accepted that the H₂O-rich fluids advecting into the mantle wedge originate from dehydration of subducted oceanic lithosphere (*e.g.*, DELANY and HELGESON, 1978; TATSUMI *et al.*, 1986). The trace element geochemistry and the isotopic composition of erupted calc-alkaline lavas along destructive plate margins demand the input of a 'slab-derived component' (*e.g.*, MORRIS *et al.*, 1990; PLANK and LANGMUIR, 1993; ISHIKAWA and NAKAMURA, 1994).

Fluids released from the subducted oceanic lithosphere are not pure H₂O, but contain various elements in solution. The original concentrations of these elements in the supercritical fluid phase depend

on the original concentrations in the source of the fluid and the partitioning coefficients between the fluid and the (partly to completely) dehydrated residual minerals of the source (*e.g.*, TATSUMI *et al.*, 1986). Additional complications arise through the interaction of slab-derived fluids with the overlying mantle during the passage from the fluid source region to the partial melting region located in the hottest part of the wedge (SCHNEIDER and EGGLEER, 1986; NAVON and STOLPER, 1988; STOLPER and NEWMAN, 1994). This process leads to mantle metasomatism, *i.e.* the trace and/or major element composition of peridotitic mantle is significantly affected by interaction with percolating fluids generated by partial dehydration of the subducting lithosphere. The typical geochemical characteristics of calc-alkaline arc magmas, the depletion of high field strength elements (HFSE) relative to the middle and heavy rare earth elements (MREE and HREE) and the enrichment of highly incompatible, very mobile elements such as large ion lithophile elements (LILE) in calc-alkaline island arc magmas are attributed to metasomatism through slab-derived fluids.

An additional process observed exclusively along convergent plate boundaries are deep-focus earthquakes with focal depths ranging from the surface down to more than 600 km. Two possible mechanisms are postulated for the generation of these earthquakes: kinetically delayed transformation of olivine to the denser spinel structure in the core of the cold subducting slab (KIRBY *et al.*, 1990; GREEN and BURNLEY, 1989) and dehydration of hydrous minerals in the downgoing slab. RALEIGH and PATERSON (1965) and MEADE and JEANLOZ (1991) identified serpentine dehydration as the principal mechanism of deep-focus earthquakes. SILVER *et al.* (1995) preferred a model whereby preserved zones of weakness in the oceanic lithosphere, *e.g.*, hydrated (serpentinized) oceanic fracture zones, were responsible for the ultradeep 1994 Bolivian earthquake.

Estimate of the H₂O-content of mantle rocks entering the subduction zone.

The potential of H₂O-transport in hydrous minerals is controlled by the following parameters: (1) the stability of hydrous minerals in a given bulk composition, (2) the modal proportions of a particular hydrous mineral in a bulk composition and (3) the extent of hydration during oceanic metamorphism. The first point is the subject of the following sections. The modal proportions of hydrous phases in completely hydrated rocks can be computed if the bulk composition and the stable mineral parageneses are known. Fully serpentinized harzburgite in the green-

schist facies entering the subduction zone contains approximately 13 wt.% H₂O stored in serpentine, brucite, chlorite and minor tremolitic amphibole. A lherzolitic composition contains less H₂O, approximately 11 wt.%, because more modal tremolite containing only about 2 wt.% H₂O is formed during the hydration. POLI and SCHMIDT (1995) and SCHMIDT and POLI (1998) have calculated the maximum H₂O content for basaltic and ultramafic compositions along typical subduction pressure-temperature paths to 240 km (8 GPa). Their calculations indicate that fully serpentinized harzburgite and lherzolite can retain over 6 wt.% H₂O at 180 km and 600°C. This is about 15 times more than basaltic (eclogitic) compositions can accommodate (0.4 wt% at 180 km, stored in lawsonite and very minor phengite). Thus, even if only minor parts (*e.g.*, local hydration along fracture zones and hydrothermal vents) of the peridotitic layer of the slab are hydrated during oceanic metamorphism it may constitute the dominant H₂O-reservoir at depths exceeding 100 km.

PHASE RELATIONS FROM FIELD DATA

The study of hydrated, serpentinized ultramafic rocks in prograde regional and contact metamorphic terrains provides a unique opportunity to extract phase equilibrium data from these rocks relevant for processes occurring during the early stages of subduction of ultramafic rocks of oceanic origin. These reactions occur at very low temperatures and are therefore very difficult to study by conventional quenching experiments. In addition, the mineralogy of low temperature serpentine is very complex and experiments of transforming one serpentine mineral (chrysotile, lizardite, and antigorite) into another in the time scale of experiments (month to years) have not been successful. The direct observation of natural parageneses in well constrained examples of progressive metamorphism enables the identification of crucial mineral reactions among the principal minerals constituting hydrated peridotites and helps to establish the succession of stable mineral parageneses.

Breakdown of serpentinite rocks as a consequence of subduction zone metamorphism may be envisaged as a process occurring in two stages. The first stage involves the transition from serpentine minerals stable at low grade, like chrysotile and lizardite, to parageneses including antigorite. The second stage comprises the stepwise, progressive breakdown of antigorite itself.

Calculated phase relations of serpentinites in the MgO-SiO₂-H₂O (MSH, relevant for harzburgitic compositions; EVANS *et al.*, 1976; SANFORD, 1981; O'HANLEY, 1991) and CaO-MgO-SiO₂-H₂O (CMSH,

relevant for lherzolitic compositions; OTERDOOM, 1978; TROMMSDORFF, 1983) systems suggest that the transition from chrysotile and lizardite to antigorite parageneses does not involve major dehydration along subduction zone geotherms (Fig. 1). The relevant, schematic reactions producing antigorite (for mineral compositions and abbreviations see Table 1)

- (1) 15 chrysotile + talc = 48 antigorite
- (2) 15 chrysotile + tremolite = antigorite + 2 diopside
- (3) 17 chrysotile = 3 brucite + antigorite

are H₂O-conserving.

Reactant and product assemblages of these reactions have been mapped (Fig. 2) in a sixty kilometer profile of prograde metamorphism along the Austroalpine boundary (TROMMSDORFF, 1983). These assemblages show wide overlap and no sharp isograds indicating sluggish reaction even in nature. Indeed, MELLINI *et al.* (1987, their Fig. 6b) demonstrated for the Malenco region (Fig. 2) with metamorphic temperatures of at least 430°C, that corroded, submicroscopic, relic inclusions of clinochrysotile are still preserved within antigorite. Nevertheless, on the basis of the assemblages observed along the Austroalpine boundary it can be safely stated that the

prograde release of aqueous fluid stored in serpentinite is not governed by the reactions that build antigorite from chrysotile. Lizardite, on the other hand, that has been mapped throughout the lower greenschist region of the profile in Fig. 2 (DIETRICH and PETERS, 1971), has not been observed in higher grade greenschist facies serpentinites, where antigorite + olivine + chlorite is common. We do not intend to discuss the question to what extent lizardite is stable (CHERNOSKY *et al.*, 1988) or metastable (c.f. O'HANLEY, 1996). From the field data in Fig. 2 it is obvious that lizardite does not play an important role in the serpentine dehydration. Lizardite is therefore not considered further in this paper. Abundant release of H₂O occurs, however, during the stepwise breakdown of antigorite and to a lesser degree of chlorite, talc and tremolite.

Antigorite, formed through reactions (1) to (3) in the pumpellyite - actinolite - chlorite zone of the greenschist facies, dominates in hydrous ultramafic rocks from upper greenschist into amphibolite facies conditions (EVANS and TROMMSDORFF, 1970; TROMMSDORFF and EVANS, 1974). Antigorite is also stable from greenschist into eclogite facies conditions (SCAMBELLURI *et al.*, 1995). The sequence of reactions that antigorite serpentinites undergo with in-

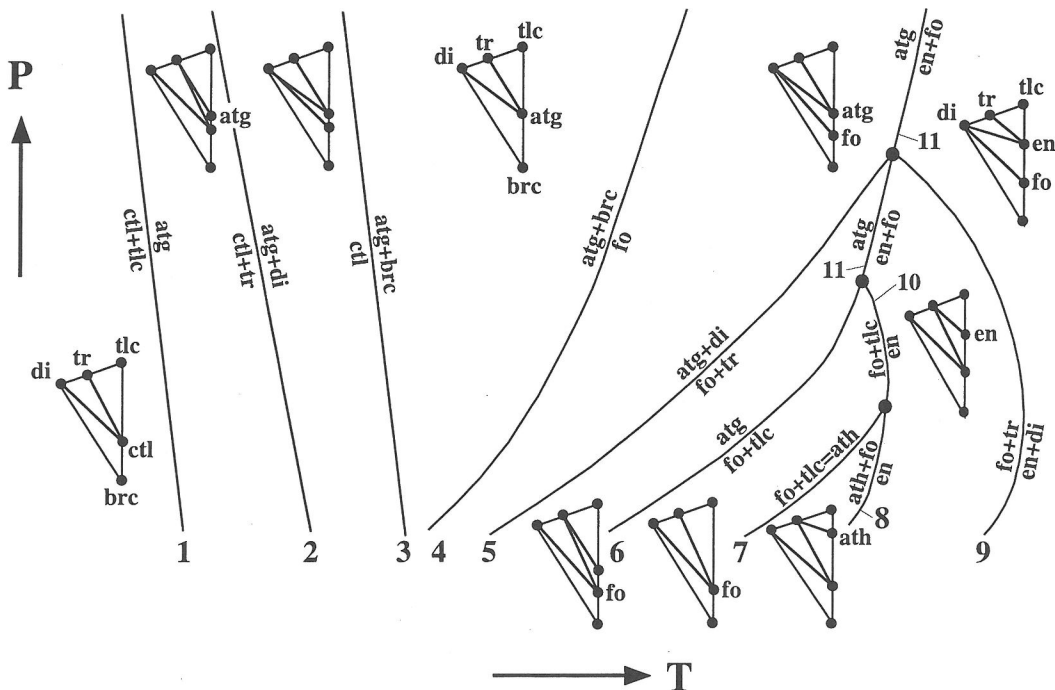


FIG. 1. Schematic representation of reactions that have been mapped in the field. Chemography is part of the projection in the CSMH tetrahedron from H₂O of the CaO-MgO-SiO₂ triangle. Diagram is not to scale and slopes of reactions are estimated but the topology satisfies field observations.

Table 1. Compositions and abbreviations of phases in the CaO-MgO-Al₂O₃-SiO₂-H₂O system, including DHMS phases

Name	Abbrev.	Formula
quartz/coesite	qtz/coe	SiO ₂
periclase	per	MgO
forsterite	fo	Mg ₂ SiO ₄
enstatite	en	MgSiO ₃
ortho-enstatite	oen	MgSiO ₃
clino-enstatite	cen	MgSiO ₃
brucite	brc	Mg(OH) ₂
serpentine (chrysotile)	srp, ctl	Mg ₃ Si ₂ O ₅ (OH) ₄
lizardite	lz	(Mg,Al) ₃ (Si,Al) ₂ O ₅ (OH) ₄
antigorite (m=17)	atg	Mg ₄₈ Si ₃₄ O ₈₅ (OH) ₆₂
talc	tlc	Mg ₃ Si ₄ O ₁₀ (OH) ₂
anthophyllite	ath	Mg ₇ Si ₈ O ₂₂ (OH) ₂
10Å-phase	10Å	Mg ₅ Si ₃ O ₁₁ (OH) ₂ ·2H ₂ O
phase A	A	Mg ₇ Si ₂ O ₈ (OH) ₆
phase E	E	Mg ₂₃ Si ₁₂ H ₂ O ₆
norbergite	nrb	Mg ₃ Si ₄ O ₁₀ (OH) ₂
chondrodite	chn	Mg ₅ Si ₃ O ₁₀ (OH) ₂
humite	hu	Mg ₇ Si ₈ O ₂₂ (OH) ₂
clinohumite	chu	Mg ₅ Si ₃ O ₁₀ (OH) ₂
diopside	di	CaMgSi ₂ O ₆
tremolite	tr	Ca ₂ Mg ₅ Si ₈ O ₂₂ (OH) ₂
chlorite (clinocllore)	chl	Mg ₅ Al ₂ Si ₄ O ₁₀ (OH) ₈
spinel	spl	MgAl ₂ O ₄
pyrope	prp	Mg ₃ Al ₂ Si ₃ O ₁₂
corundum	crn	Al ₂ O ₃
diaspore	dsp	AlO(OH)
MgMgAl-pumpellyite	pmp	Mg ₄ (Al,Mg)Al ₄ Si ₆ O ₂₁ (OH) ₇
cordierite	crd	Mg ₂ Al ₄ Si ₂ O ₁₈
Ti-clinohumite (x=0.5)	Ti-chu	Ti _{1.5} Mg _{4.5} Si ₃ O ₁₇ (OH)
Ti-chondrodite	Ti-chn	Ti _{1.5} Mg _{4.5} Si ₃ O ₁₇ (OH)
ilmenite	ilm	(Fe,Mg)TiO ₃

DHMS - Dense Hydrous Magnesium Silicates
Abbreviations are after KRETZ (1983)

creasing temperature has been mapped in detail for the case of contact metamorphism (TROMMSDORFF and EVANS, 1972; SPRINGER, 1974; FROST, 1975; ARAI, 1975; MATTHES and KNAUER, 1981) and for intermediate pressure regional metamorphism (TROMMSDORFF and EVANS, 1974). In order of increasing grade the following assemblages have been observed in these field studies: antigorite + brucite + diopside; antigorite + olivine + diopside; antigorite + olivine + tremolite; olivine + talc + tremolite; olivine + magnesian amphibole (anthophyllite and/or Mg-cummingtonite) + tremolite; olivine + enstatite¹ + tremolite; olivine + enstatite + diopside. Chlorite has been observed throughout the sequence and reacts at higher grades continuously to form spinel (see EVANS and FROST, 1975). From mapping these assemblages, a sequence of stable reac-

¹ Throughout this paper the term enstatite is used for both clino- and ortho-enstatite, as it is often not specified in the original publications what type of enstatite is observed either in the field or in the experiments. The transformation from ortho- to high-clinoenstatite (C2/c) occurs between 6.5 GPa at 500°C and 7.5 GPa at 800°C (PACOLO and GASPARIK, 1990; ANGEL *et al.*, 1992) and is associated with approximately 3% volume change. At low temperatures (≤600°C) and pressures from 0 to 6.5 GPa, low-clinoenstatite (P2₁c) is stable which shows very minor volume difference (0.15%) to orthoenstatite.

tions may be established for ultramafic rocks in the CSMH system. These reactions are from low to high grade (Fig. 1):

- (4) antigorite + 20 brucite = 34 forsterite + 51 H₂O
- (5) antigorite + 8 diopside = 18 forsterite + 4 tremolite + 27 H₂O
- (6) antigorite = 18 forsterite + 4 talc + 27 H₂O
- (7) 4 forsterite + 9 talc = 5 Mg-amphibole + 4 H₂O
- (8) Mg-amphibole + forsterite = 9 enstatite + H₂O
- (9) forsterite + tremolite = 5 enstatite + 2 diopside + H₂O.

The prograde sequence up to reaction (8) corresponds to sharply defined isograds in contact meta-

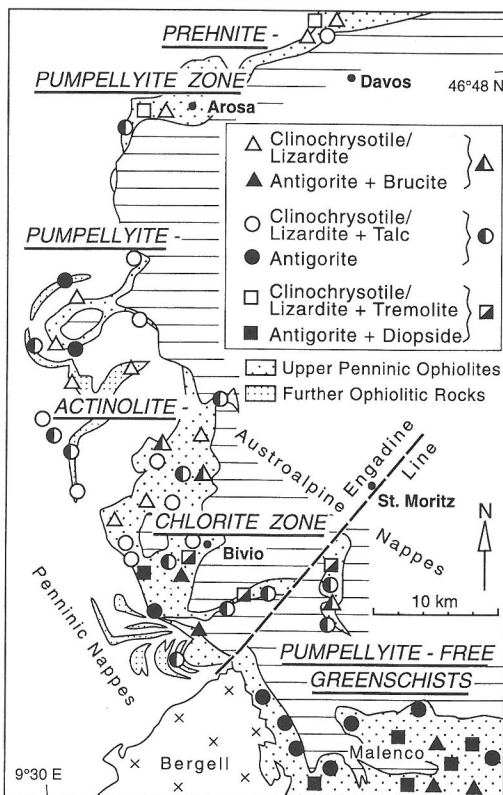
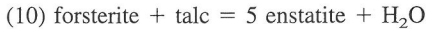


Fig. 2. Distribution of serpentinite mineral assemblages along the Penninic-Austroalpine boundary region, Swiss and Italian Alps (after TROMMSDORFF, 1983). Product and reactant assemblages of reactions 1 (circles), 2 (squares), and 3 (triangles) are overlapping in wide areas. The transition from chrysotile and lizardite to antigorite parageneses occurs over a distance of several tens of kilometers from prehnite-pumpellyite facies into greenschist facies conditions.

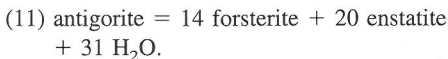
morphism (TROMMSDORFF and EVANS, 1972; FROST, 1975). For the regional metamorphism of the Central Alps (TROMMSDORFF and EVANS, 1974, their Figs. 4–6) a wide overlap in the distribution of forsterite + talc, forsterite + Mg-amphibole and forsterite + enstatite is observed. Furthermore, for the same area EVANS and TROMMSDORFF (1974) gave proof that the reaction



has also taken place.

This reaction is favoured in Fe-poor ultramafic rocks relative to reaction (7) or, alternatively, by high pressure. Calculations by EVANS and GUGGENHEIM (1988) showed that some MSH equilibria involving Mg-amphibole and enstatite are considerably displaced by substitution of Fe for Mg in amounts typical for ultramafic rocks. There, the stability field for Mg-amphibole is expanded from 0.6 to over 1.1 GPa. Thus, some of the overlap of the distribution in assemblages of ultramafic rocks in the Central Alps may be due to variations in bulk composition, and some to variations in fluid composition. In addition, as Mg-amphibole is always late in the area it may largely have formed on the retrograde path of the P-T loop and the actual prograde reaction was (10).

Under even higher pressure conditions, no stability field for forsterite + talc exists any more. The transition from antigorite rocks to forsterite + enstatite rocks then occurs according to the reaction:



So far, this reaction has been demonstrated only at one locality. It was mapped in an eclogite facies terrain of the Sierra Nevada, southern Spain by TROMMSDORFF *et al.* (1998). The pressure estimates for these rocks are in excess of 2.0 GPa and 650°C.

The entire information described above may now be used to construct a schematic pressure-temperature diagram for CMSH phases and typical lherzolitic to harzburgitic serpentinite compositions, taking into account entropy and volume data of the phases involved (Fig. 1). Strictly speaking, this phase diagram topology is only valid for mineral compositions encountered in the field, but thermodynamically derived phase diagrams and experimental data *must* be consistent with this field topology. Figure 3 is the calculated phase diagram using the BERMAN (1988) database. This field and thermodynamically based phase diagram calculation can be used as a basis for extrapolations to higher, inaccessible P-T regions. An interesting feature of Fig. 3 are the relative stability fields of Mg-amphibole + forsterite, talc + forsterite and tremolite + forsterite.

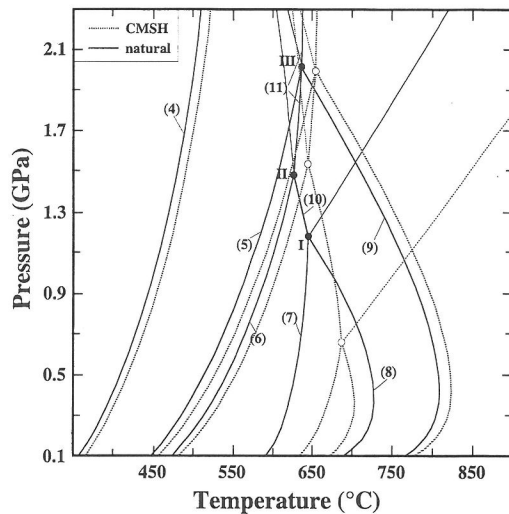
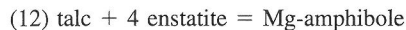


FIG. 3. Phase diagram calculated for reactions in the CMSH system using the BERMAN (1988) database (dotted lines, open circles). Numbers refer to reactions listed in the text. Solid lines and dots correspond to the same equilibria if substitution of Fe for Mg is taken into account in amounts typical for metamorphosed ultramafic rocks (x_{Fe} for ol = 0.89; en = 0.90; tlc = 0.97; ath = 0.88; atg = 0.95; brc = 0.91; tr = 0.95; di = 0.96). Thick lines correspond to reactions that have been mapped in the field, thin lines to other reactions. The topology of the phase diagram is identical to that derived from the field (Fig. 1) and does not change with substitution of Fe for Mg. Note that the diagram is approximate because the influence of trivalent cations is not taken into account. They will stabilize atg and amphibole.

These fields envelop each other and close towards high pressures at invariant points which are aligned along reactions bounding the stability field for enstatite + forsterite + H₂O. Two of these invariant points, namely I and III, may provide valuable bathogrades (CARMICHAEL, 1991) for hydrous ultramafic rocks, because their position is relatively insensitive to substitutions of Fe²⁺ for Mg (Fig. 3). Point I, on the other hand, involves the H₂O conserving reaction:



and is quite sensitive to pressure as a response to Fe-presence in the silicate phases (EVANS and GUGGENHEIM, 1988). It seems, however, that the displacement of any of the equilibria 1–12 caused by the substitution of Fe²⁺ for Mg is insufficient to create a new topology of the pure CMSH phase diagram compared to the field-derived topology (Fig. 3).

A further departure from the pure CMSH system may be found in all equilibria in which participating phases contain significant amounts of aluminum. Antigorite, that can take up to 5 wt.% Al₂O₃, actually

breaks down to forsterite + talc + chlorite (TROMMSDORFF and EVANS, 1974, p. 64) and at high pressures to forsterite + enstatite + chlorite (TROMMSDORFF *et al.*, 1998). The amount of Mg-chlorite produced by these reactions is, for antigorite with 5 wt.% Al_2O_3 , in the order of 20–30 mole % Mg-clinochlore. At ≈ 2 GPa the breakdown of clinochlore to enstatite + olivine + spinel or to olivine + garnet + spinel occurs at $\approx 150^\circ\text{C}$ above the antigorite breakdown (FAWCETT and YODER, 1966; STAUDIGEL and SCHREYER, 1977; JENKINS and CHERNOSKY, 1986; FOCKENBERG, 1995). Thus the release of about 25% of the H_2O stored in an aluminium-bearing serpentinite is spread out over that temperature interval (see also SCHMIDT and POLI, 1998).

Finally, titanium hydroxyl-clinohumite occurs quite commonly in antigorite serpentinites at low metamorphic grade (greenschist facies conditions). Although it breaks down to olivine plus ilmenite at low pressures near the isograd corresponding to reaction (5) (TROMMSDORFF and EVANS, 1980) it persists to eclogite conditions along cool geotherms (SCAMBELLURI *et al.*, 1995, ZHANG *et al.*, 1995). As a carrier of H_2O to mantle depth, titanian hydroxyl-clinohumite is, however, quantitatively unimportant.

EXPERIMENTAL DATA BEARING ON THE PHASE RELATIONS OF ULTRAMAFIC MANTLE COMPOSITIONS AT HIGH PRESSURES

Field studies show (see section 2) that the serpentine mineral antigorite is the most important hydrous phase at upper greenschist to eclogite or amphibolite facies conditions in ultramafic compositions. The phase relations of antigorite control the H_2O -budget at the initiation of subduction. The breakdown of antigorite and the formation of 'post-antigorite' hydrous phases will be the dominant control of H_2O -transport in deeper parts of the subducting oceanic lithosphere. Therefore, the discussion of hydrate stability in subducting ultramafic compositions starts with a summary of high-pressure phase relations of serpentine minerals. The following "boundary conditions" based on field observations must be considered if phase equilibrium experiments at high pressures in the ultramafic system are to be used for the construction of phase diagrams relevant for the stability and breakdown of hydrous phases in subduction zones:

Antigorite is the stable serpentine mineral at elevated pressures and temperatures. All field studies on the progressive metamorphism of hydrated ultramafic mantle rocks revealed that chrysotile and lizardite are participating in the breakdown reaction of serpentine at their stability limit, but transform to antigorite at lower to middle greenschist facies conditions (300–

350°C) within the stability field of serpentine + brucite (EVANS *et al.*, 1975) (reaction (3), Fig. 1). Therefore, all experimental studies using chrysotile or lizardite starting materials (natural or synthetic) or delimiting the serpentine stability field from synthesis experiments resulting in chrysotile or lizardite could represent metastable assemblages with respect to antigorite bearing parageneses. The considerable discrepancy between the stability and the phase relations of serpentine-bearing assemblages at high pressures among the different experimental studies can partly be related to this fundamental difference in the serpentine mineralogy.

The only known example of antigorite breakdown under eclogite facies conditions (Sierra Nevada, Spain, TROMMSDORFF *et al.*, 1998) reveals that antigorite cannot be represented in the MSH system, but contains considerable amount of Al, corresponding to more than 0.25 mole fraction of clinochlore dissolved in the antigorite structure. Aluminium is known to decrease the c-value in both the tetrahedral (Si, Al) and octahedral (Mg, Al) sheets in the corrugated antigorite structure (UEHARA and SHIROZU, 1985) and most probably increases the stability of antigorite. Cr and Fe^{3+} , which can be present in natural antigorites in appreciable amounts, could stabilize the antigorite structure even further. Experiments in pure MSH, provided that pure MSH antigorite can indeed be synthesized (see below), possibly result in an antigorite stability field considerably smaller than in nature, where Al, Fe^{3+} and Cr are always present in ultramafic mantle compositions. As a consequence of the high Al-content, antigorite breakdown is accompanied by chlorite growth retaining some of the original H_2O (up to 25%) in hydrous phases.

The high-pressure stability of serpentine minerals will be discussed separately in the two following sections: Chrysotile and lizardite experiments and antigorite experiments.

High pressure experiments on chrysotile and lizardite stability

The presentation of phase equilibrium studies of chrysotile and lizardite in this contribution is limited to pressures exceeding 0.5 GPa. Numerous studies exist at low pressures, starting with the pioneering work of BOWEN and TUTTLE (1949) on chrysotile stability in the pure MSH system and YODER (1952) on the stability of aluminous lizardite in the MASH system. Most of these studies were synthesis experiments on various compositions to delimit the stability of brucite + serpentine and of the serpentine alone. Excellent summaries of these low-pressure phase relations are provided by the paper of CHER-

NOSKY *et al.* (1988) and the book by O'HANLEY (1996).

Figure 4 depicts a summary of the high-pressure phase relations for the two serpentine group minerals chrysotile and lizardite. The major difference from the field derived phase diagram (Figs. 1 and 3) is the lack of the direct breakdown of serpentine to the anhydrous assemblage forsterite + enstatite + H₂O, corresponding to reaction (11). Instead a transformation corresponding to reaction (6),



has been observed for a wide pressure range from 0.05 GPa (*e.g.*, BOWEN and TUTTLE, 1949; CARUSO and CHERNOSKY, 1979; CHERNOSKY, 1982) to pressures as high as 6 GPa (PISTORIUS, 1963; KITAHARA *et al.*, 1966; YAMAMOTO and AKIMOTO, 1977; KHODYREV and AGOSHKOV, 1986). Below 4–5 GPa the talc + forsterite stability field is bound by reaction (10); Mg-amphibole was not observed in the experimental studies cited above. The solid lines in Fig. 4 represent

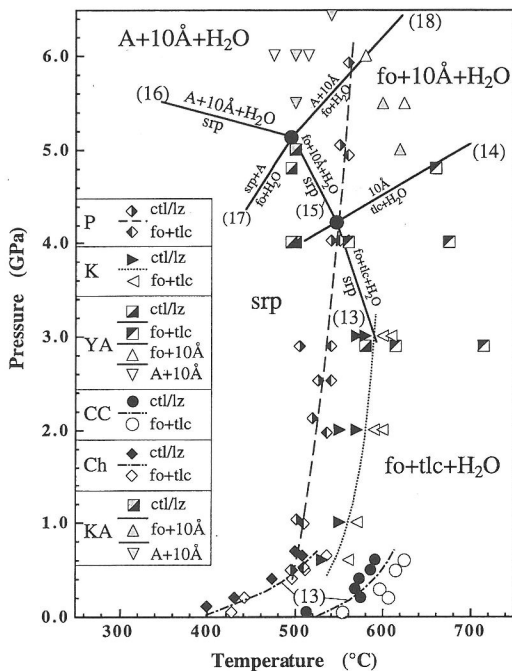
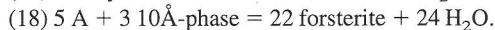
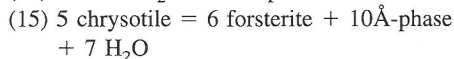
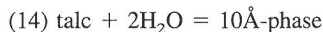


FIG. 4. Summary of experimental data points involving the serpentine (srp) minerals chrysotile (ctl) and lizardite (lz) and product phases forsterite (fo), talc (tlc), enstatite (en), 10 Å phase (10Å) and phase A (A). Experiments are from P - PISTORIUS (1963); K - KITAHARA *et al.* (1966); YA - YAMAMOTO and AKIMOTO (1977); CC - CARUSO and CHERNOSKY (1979); Ch - CHERNOSKY (1982); KA - KHODYREV and AGOSHKOV (1986). Experimental fits are eyeball fits with numbers corresponding to reactions listed in text and Table 2.

a 'petrogenetic grid' compatible with experimental results from YAMAMOTO and AKIMOTO (1977) and KHODYREV and AGOSHKOV (1986). Only reaction boundaries observed in a "mantle bulk composition", i.e. compositions bounded by the assemblage forsterite - enstatite - H₂O in the MSH system are drawn. Reactions only affecting compositions that are either more magnesian (to the left of the forsterite-H₂O join on Fig. 5) or more silica-rich than the enstatite - H₂O join have been omitted for clarity.

The experimental brackets of KITAHARA *et al.* (1966), YAMAMOTO and AKIMOTO (1977) and KHODYREV and AGOSHKOV (1986) are consistent. The results of the lower pressure studies of CHERNOSKY (1982) and CARUSO and CHERNOSKY (1979) have been added to Fig. 4 to emphasize the importance of the starting material investigated. CHERNOSKY (1982) used synthetic chrysotile in the MSH system. The experimental brackets are consistent with the work of BOWEN and TUTTLE (1949) and nearly consistent with the high-pressure investigation of KITAHARA *et al.* (1966) using a similar synthesis technique for chrysotile. CARUSO and CHERNOSKY (1979) investigated the breakdown of synthetic aluminous lizardite, containing 0.5 clinocllore-component corresponding to the chemical formula Mg_{5.5}Al_{1.0}Si_{3.5}O₁₀(OH)₈. Aluminum clearly stabilizes the serpentine mineral; the difference between the two curves (pure chrysotile and aluminous lizardite) is in the order of 120°C.

At high pressures, various parageneses are observed along the serpentine breakdown curve and beyond. The stability of post-serpentine DHMS phases will be discussed in more detail later. In short, the phase assemblages involving the 10Å-phase (BAUER and SCLAR, 1981) and phase A (RINGWOOD and MAJOR, 1967) observed by YAMAMOTO and AKIMOTO (1977) and KHODYREV and AGOSHKOV (1986) are consistent with each other and with the reaction boundaries drawn on Fig. 4. The following reactions can be deduced from the assemblages they observed:



High-pressures experiments on antigorite stability

Experimental studies on the stability of antigorite and its breakdown products have been difficult, because successful synthesis of antigorite in the MSH system has only very rarely been achieved (ISHII and SAITO, 1973; JOHANNES, 1975; WUNDER *et al.*, 1997).

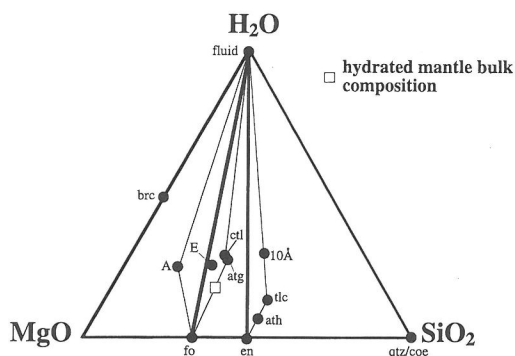


FIG. 5. Chemographic representation of phases in the system $\text{MgO-SiO}_2\text{-H}_2\text{O}$. Abbreviations are listed in Table 1. The hydrated mantle bulk composition is given for maximum hydration. It moves with increasing dehydration away from the H_2O apex.

ISHII and SAITO (1973) produced antigorite from silica-rich alkaline solutions under low excess H_2O conditions in a pure MSH system; JOHANNES (1975) grew antigorite from an oxide mix with seeds of Fe,Al-bearing natural antigorite in very long runs. WUNDER *et al.* (1997) used presynthesized brucite and talc as starting material and run durations of 5 days at 5 GPa and 500°C ; the product consisted of antigorite plus minor chrysotile and brucite or talc. This mixture was later used in the study of WUNDER and SCHREYER (1997) on the stability of antigorite.

A summary of available phase equilibrium data on the stability of antigorite and its breakdown products is shown in Fig. 6. EVANS *et al.* (1976) used mixtures of natural Al- and Fe-bearing antigorite and synthetic forsterite and talc. Their study was aimed at delimiting the breakdown of antigorite to forsterite + talc + H_2O (reaction (6)) up to 1.5 GPa. The growth of antigorite at low pressures was very sluggish and they concluded that the breakdown reaction has to occur to the high temperature side of their bracketing experiments. Many experiments, in particular at low pressures (and temperatures), did not result in conclusive changes of the mineral assemblages (see Fig. 6). EVANS *et al.* (1976) performed the first comprehensive study on antigorite stability and observed a higher temperature stability of antigorite than for either chrysotile or low-Al lizardite (see above, Fig. 4). At 1 GPa the difference is $\approx 90^\circ\text{C}$. ULMER and TROMMSDORFF (1995), WUNDER and SCHREYER (1997), and BOSE and NAVROTSKY (1998) extended this study to higher pressures. ULMER and TROMMSDORFF (1998) used natural, well crystallized antigorite with a homogeneous periodicity of $m = 17$ which contains approximately 2 wt.% of combined Al, Fe^{3+} , and Cr. The breakdown of antigorite up to 8

GPa was investigated with a similar technique as by EVANS *et al.* (1976): Natural antigorite + brucite was mixed with 10% olivine + enstatite. WUNDER and SCHREYER (1997) used two different starting materials: (1) mixtures of synthetic MSH antigorite, forsterite, enstatite, and 20 wt.% H_2O and (2) mixtures of natural antigorite, containing approximately 1.7 wt.% trivalent cations, forsterite, enstatite, and H_2O . Figure 6 reveals a considerable, yet unresolved, discrepancy between the two experimental determinations of the high-pressure stability of antigorite. Up to 4 GPa WUNDER and SCHREYER'S (1997) (WS) curve for reaction (11) is approximately 40°C below that of ULMER and TROMMSDORFF (1995); at higher pressure the WS curve sharply bends into a strongly negative slope so that the difference becomes 100°C at 5 GPa. As a consequence, in the case of WUNDER and SCHREYER (1997), exceedingly cold subduction paths of 500°C at 5 GPa (160 km) would be necessary to carry any H_2O in ultramafic rocks deeper than this "choke point" (KAWAMOTO *et al.*, 1995) of complete dehydration of antigorite to forsterite plus enstatite. Only chlorite, accommodating the Al-component in the peridotite, could possibly survive to high temperatures (see the section on chlorite). In the case of ULMER and TROMMSDORFF (1995), the "choke point" is located around 6 GPa and 600°C , where antigorite transforms to other hydrate-bearing assemblages containing phase A and possibly the 10\AA phase. BOSE and NAVROTSKY (1998) have performed a similar study in a restricted pressure - temperature interval (Fig. 6). They conducted reversal experiments with mixtures of natural antigorite and synthetic forsterite, enstatite and phase A. Their results on the breakdown of antigorite compare within experimental error (approximately $\pm 15^\circ\text{C}$ and 0.2 GPa in a multi-anvil apparatus) with ULMER and TROMMSDORFF (1995). The major difference between the two studies is the interpretation of the stability or metastability of the 10\AA -phase: BOSE and NAVROTSKY (1998) consider the 10\AA -phase as metastable and, consequently, they only propose equilibria involving antigorite, phase A, enstatite, and forsterite at pressures exceeding the forsterite plus talc stability field. From the following observations we conclude that the 10\AA -phase forms part of the stable phase assemblage in a narrow P-T interval between 5.5 and 7.5 GPa and $< 630^\circ\text{C}$ just above the antigorite breakdown: (1) ULMER and TROMMSDORFF (1995) have reported abundant 10\AA -phase in their experimental charges at pressures between 5.5 and 7.0 GPa just below and above the breakdown of antigorite. (2) An additional reversal experiment performed by the authors at 6 GPa/ 620°C (48 hrs.), starting with a 1:1 mixture of natural antigorite + brucite and Phase A + enstatite (synthe-

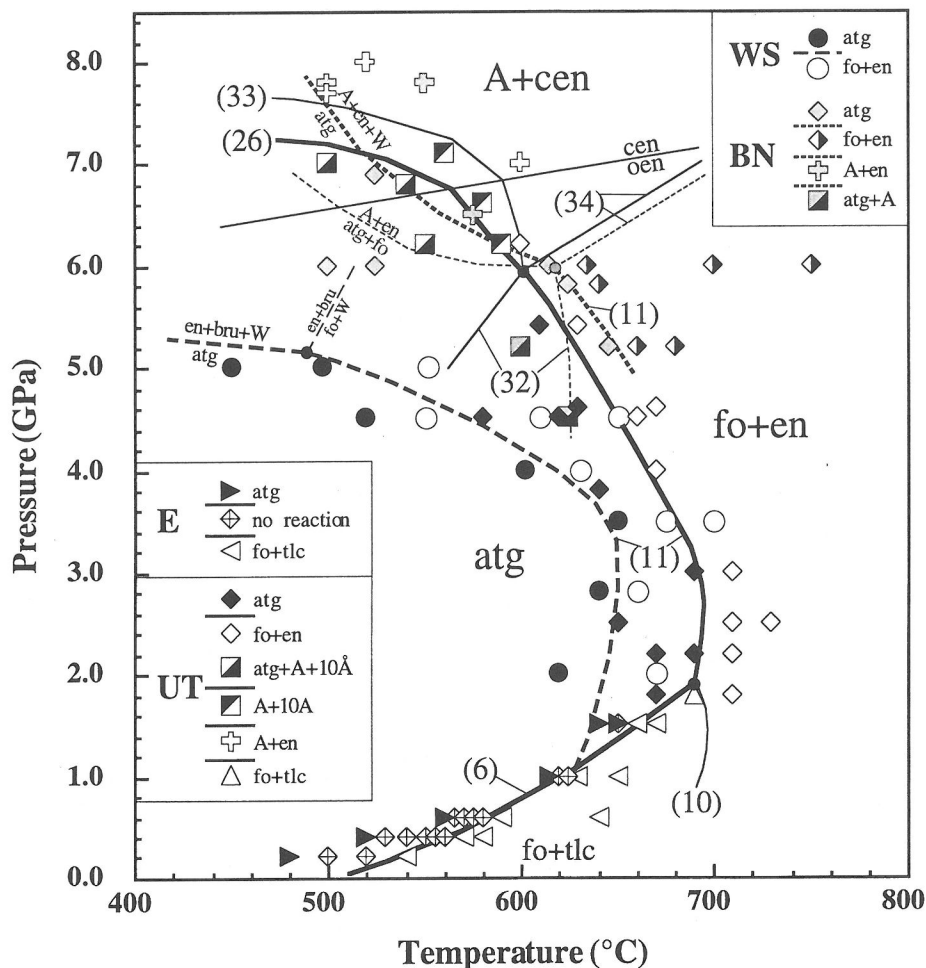


FIG. 6. Summary of experimental data points involving breakdown of antigorite. Mineral abbreviations are listed in Table 1; W = H₂O-fluid. Experimental fits are eyeball fits of data by E - EVANS *et al.* (1976); UT - ULMER and TROMMSDORFF (1995); WS - WUNDER and SCHREYER (1997), and BOSE and NAVROTSKY (1998). The phase transition from orthoenstatite (oen) to high-clinoenstatite (cen) (PACOLO and GASPARIK, 1990, ANGEL *et al.*, 1992) is indicated. Numbers of reactions are listed in the text and Table 2.

sized from natural antigorite + brucite at 8 GPa/700°C), resulted complete transformation to the assemblage forsterite + 10Å-phase + H₂O. (3) A TEM/SEM analysis of the run products of ULMER and TROMMSDORFF (1995) revealed that the 10Å-phase forms large (up to 50 mm) euhedral crystals unlike 'normal' quench crystals (see section 3.5 for further discussion).

High pressure experiments on the stability of the assemblage forsterite + talc

A second important "choke point" is invariant point II, terminating the stability field of forsterite +

talc. The experimental brackets of the reversal experiments by KITAHARA *et al.* (1966), GUGGENBUEHL (1994) and PAWLEY (1998) for reaction (10), forsterite + talc = enstatite + H₂O, are presented in Fig. 7. Additional experiments to delimit this reaction have been performed by YAMAMOTO and AKIMOTO (1977), ULMER and TROMMSDORFF (1995) and WUNDER and SCHREYER (1997). KITAHARA *et al.* (1966) used pre-synthesized talc, forsterite and enstatite, as well as oxide mixtures; GUGGENBUEHL (1994, unpublished Diploma thesis performed at ETH Zurich) and PAWLEY (1998) used synthetic forsterite, enstatite and talc as well as natural talc. Despite similar experimental

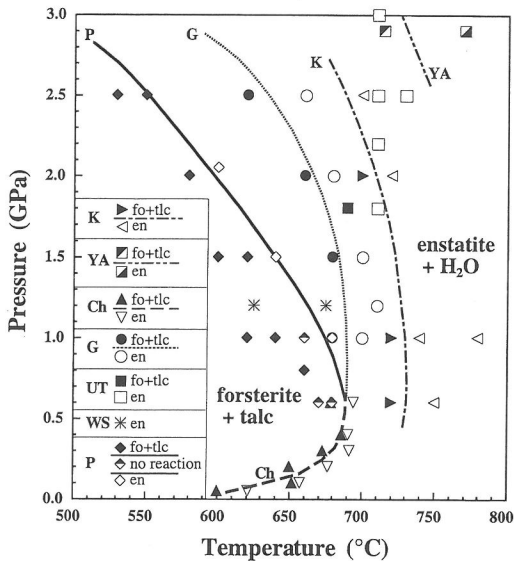


FIG. 7. Summary of experimental data points for the reaction (10) forsterite + talc = 5 enstatite + H₂O. Mineral abbreviations are listed in Table 1. Experimental fits are eyeball fits of data by K - KITAHARA *et al.* (1966), YA - YAMAMOTO and AKIMOTO (1977), Ch - CHERNOSKY *et al.* (1985); G - GUGGENHEIM (1994); UT - ULMER and TROMMSDORFF (1995); WS - WUNDER and SCHREYER (1997); and P - PAWLEY (1998).

techniques used by the various investigators, enormous discrepancies exist in the location of reaction (10) in P-T space. The preliminary, reversed experiments of GUGGENBUEHL (1994) revealed a lower temperature stability of forsterite + talc and its metastable extension into the antigorite stability field than in the experiments of KITHARA *et al.* (1966). The difference between GUGGENBUEHL (1994) and KITAHARA *et al.* (1966) is approximately 40°C at 2 GPa. The experimental brackets obtained by PAWLEY (1998) are considerably lower than all previous studies: The difference to GUGGENBUEHL (1994) is about 70°C at 2 GPa. This results in a smaller stability field for forsterite + talc, reducing the significance of talc as a potential H₂O-carrier in subduction zones even further.

BERMAN *et al.* (1986) considered the experiments by KITAHARA *et al.* (1966) as metastable due to the short run times and the fine-grained poorly crystallized starting material (it is, however, not clear why this would favor the hydrate assemblage over the anhydrous enstatite); in addition these experiments are not consistent with the low pressure brackets obtained by CHERNOSKY *et al.* (1985) for reaction (10). The experimental curves derived by GUGGENBUEHL (1994) and PAWLEY (1998) are compatible with

the low-pressure brackets determined by CHERNOSKY *et al.* (1985).

The experimental studies of KITAHARA *et al.* (1966), GUGGENBUEHL (1994), and PAWLEY (1998) on the reaction talc + forsterite = enstatite + H₂O (Fig. 7) were all performed with similar starting materials (synthetic and natural talc, synthetic forsterite and enstatite), all were reversal not synthesis experiments and produced as much as 140°C difference at 2.5 GPa. The only likely explanations we can offer do date are possible differences in the activity of H₂O in the different experimental studies.

The synthesis experiments of YAMAMOTO and AKIMOTO (1977) inferred reaction (10) to be located at even higher temperatures than the brackets of KITAHARA *et al.* (1966); at 2.9 GPa/715°C they still observed forsterite + talc.

Reaction (10), is metastable with respect to Mg-amphibole at low pressures (see Fig. 3, reactions (7) and (8)). It is possible to study the metastable extension of reaction (10) to low pressures (CHERNOSKY *et al.*, 1985), due to the extremely sluggish nucleation of Mg-amphibole in the MSH system. Mg-amphibole has been omitted in Fig. 6 because its stability field is not relevant for subduction. It is only stable under low pressure - high temperature amphibolite to granulite facies conditions not encountered during subduction zone metamorphic conditions.

In conclusion the phase relations depicted in Figs. 6 and 7 for the stability and breakdown of antigorite serpentine and the assemblage forsterite + talc are not yet consistent. Difficulties in the synthesis of antigorite in the pure MSH system and the well known persistence of talc (*e.g.*, EVANS and GUGGENHEIM, 1988) in both pressure and temperature makes this system one of the most difficult ones to study and represents a real challenge to experimental petrology. A fundamental question regarding the experimental determination of the phase topologies in the MSH system is its applicability to ultramafic mantle compositions. Only if the topologies and approximate locations of the reaction boundaries coincide with field-constrained parageneses should one attempt to apply the MSH system to mantle rocks. The absence of the direct breakdown of serpentine to form olivine + enstatite (reaction (11)) in the chrysotile and lizardite experiments (PISTORIUS, 1963; KITAHARA *et al.*, 1966; YAMAMOTO and AKIMOTO, 1977; KHODYREV and AGOSHKOV, 1986) is not consistent with field observations, which demonstrate that chrysotile and lizardite transform to antigorite at low temperatures followed by the direct reaction of (antigorite) serpentine to olivine + enstatite + chlorite at pressure exceeding 2 GPa (TROMMSDORFF *et al.*, 1998). The general topology of the antigorite phase diagram

(Fig. 6) with a talc-forsterite field closing between 1.5 and 2 GPa (according to GUGGENBUEHL, 1994 and PAWLEY, 1998) is consistent with field observations and will be used to construct a "petrogenetic grid" for hydrous mantle rocks in section 3.5 (Fig. 11).

The experiments performed by EVANS *et al.* (1976), CHERNOSKY *et al.* (1985), GUGGENBUEHL (1994), ULMER and TROMMSDORFF (1995), BOSE and NAVROTSKY (1998), and PAWLEY (1998) and repeat experiments at 690°C and 710°C at 1.8 GPa² in an endloaded piston cylinder apparatus (BOYD and ENGLAND, 1960) by the authors permit the drawing of a consistent phase diagram in which invariant point II is placed at approximately 680°C and 1.8 GPa (Figs. 6 and 11). It has, however, to be stressed that perfect accordance between MSH experiments (KITAHARA *et al.*, 1966; CHERNOSKY *et al.*, 1985; GUGGENBUEHL, 1994; WUNDER *et al.*, 1997; PAWLEY, 1998) and the natural system (EVANS *et al.*, 1976; ULMER and TROMMSDORFF, 1995; BOSE and NAVROTSKY, 1998) is neither necessary nor expected. The presence of Fe²⁺ and its fractionation between the various silicate phases can account for as much as 20°C difference in the reaction temperatures alone (Fig. 3). The effect of trivalent cations on the stability of antigorite has not been studied yet. Antigorite can contain several wt.% Fe₂O₃ (O'HANLEY, 1996) up to 5 wt.% Al₂O₃ and up to 0.5 wt.% Cr₂O₃ (TROMMSDORFF and EVANS, 1974; TROMMSDORFF *et al.*, 1998). However, it is very unlikely that the presence of moderate amounts of additional oxide components (in the order of 0.1 to 1 wt%) will affect the phase equilibria by as much as 100°C or more.

High pressure phase relations of post-serpentine phases

The stability of hydrous phases other than serpentine and talc is summarized in Fig. 8. The compilation includes the available phase equilibrium data from KITAHARA *et al.* (1966), YAMAMOTO and AKIMOTO (1977), KHODYREV and AGOSHKOV (1986), LUTH (1995), ULMER and TROMMSDORFF (1995), KAWAMOTO *et al.* (1995), IRIFUNE *et al.* (1998), WUNDER (1998), and BOSE and NAVROTSKY (1998). In addition to the main phase fields delimited on Fig. 8, humite phases, such as hydroxyl-clinohumite and hydroxyl-chondrodite have been observed by LUTH (1995) and KAWAMOTO *et al.* (1995). The solid phase boundaries

are drawn according to the experimental information available in this system for bulk compositions restricted to the range $2 > \text{Mg/Si} > 1$, i.e. between forsterite and enstatite. This corresponds to the compositional range of mantle peridotites expressed in Mg/Si ratios. This restriction excludes humite and other low silica DHMS phases at low pressures when the forsterite-H₂O join is stable (compare Fig. 5) and the occurrence of talc/10Å-phase to conditions where the enstatite - H₂O join is not stable. The dashed lines confirm with the experimental results of LUTH (1995) on the stability of phases A and E.

Despite the difference in starting materials and experimental procedures, the consistency of the available experimental data at low temperatures is very good. The phase fields for the parageneses forsterite + 10Å-phase, phase A + 10Å-phase, and phase A + enstatite are consistent among the work of YAMAMOTO and AKIMOTO (1977), KHODYREV and AGOSHKOV (1986), ULMER and TROMMSDORFF (1995), and BOSE and NAVROTSKY (1998) and the phase equilibrium study on the talc-10Å-phase relationship by PAWLEY and WOOD (1995).

The major discrepancies among the different experimental studies concern the stability of phases A and E (KANZAKI, 1991) at temperatures exceeding 700°C: The study of LUTH (1995) resulted in a larger stability field for phase A than the studies of IRIFUNE *et al.* (1998) and WUNDER (1998) and a smaller stability field for phase E than KAWAMOTO *et al.* (1995) and IRIFUNE *et al.* (1998).

KAWAMOTO *et al.* (1995) used a natural starting material containing Fe, Al, Cr (very fertile peridotite KLB-1) and reported high Al₂O₃-contents of phase E (up to 9 wt.%). Aluminum should stabilize phase E relative to phase A + enstatite, because the latter contains only very little Al₂O₃ (≤ 0.25 wt%). This could indicate that phase E is more important in the earth's mantle than anticipated from the pure MSH system (similar to antigorite). WUNDER (1998) proposed that the reduced temperature stability of the assemblage phase A + enstatite compared with LUTH (1995) is the result of different polymorphs of clinoenstatite used in their experimental studies (low-P clinoenstatite by WUNDER; high-P clinoenstatite by LUTH). This discrepancy, however, cannot be reconciled completely to date and the phase boundaries

² Starting materials	apparatus	run duration	P	T	result
atg, brc, fo, en	piston cylinder	100 hrs.	1.8 GPa	690°C	atg, fo, tlc
atg, brc, fo, en	piston cylinder	100 hrs.	1.8 GPa	710°C	oen, fo, chl, \pm tlc

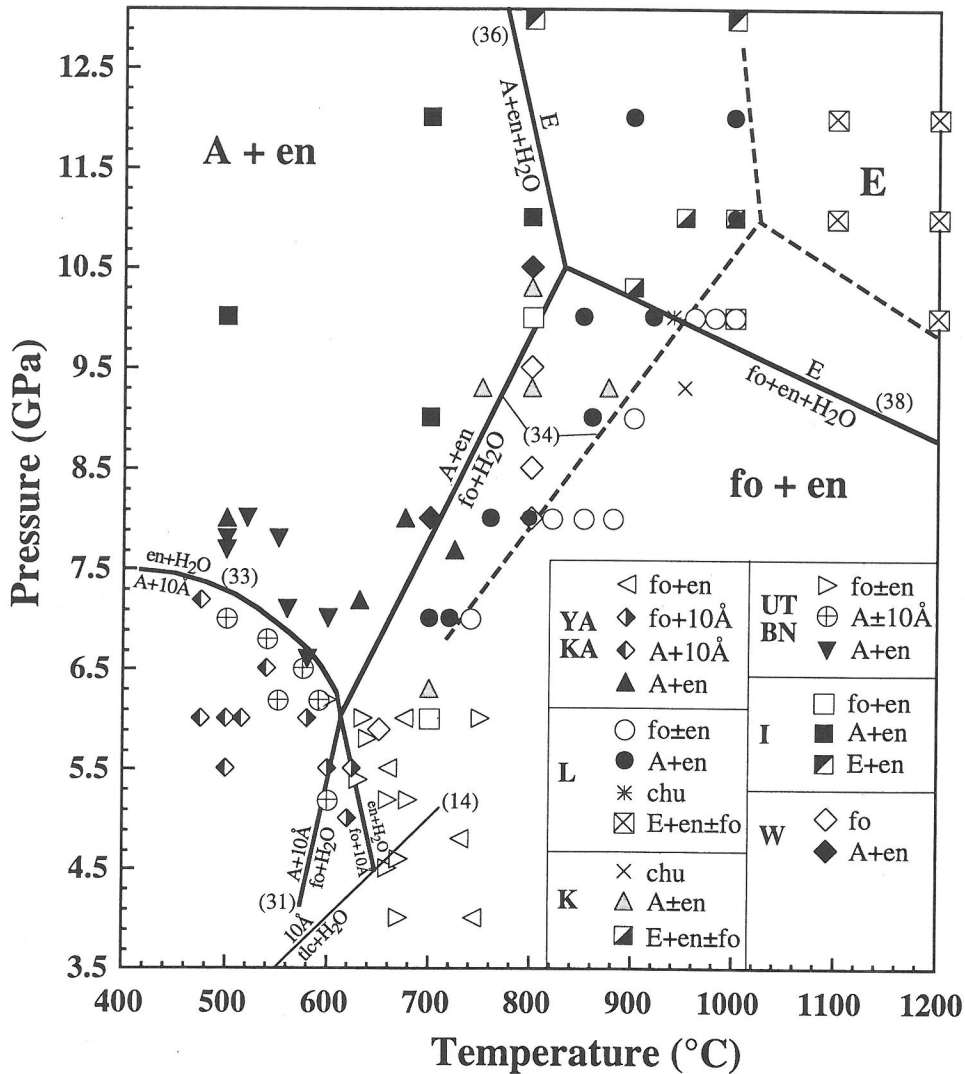


FIG. 8. Summary of experimental data points involving phases above the breakdown of serpentine minerals. Mineral abbreviations are listed in Table 1. Experimental curves are eyeball fits of data by YA - YAMAMOTO and AKIMOTO (1966); KA - KODYREV and AGOSHKOV (1986); L - LUTH (1995); K - KAWAMOTO *et al.* (1995); UT - ULMER and TROMMSDORFF (1995); I - IRIFUNE *et al.* (1998), BN - BOSE and NAVROTSKY (1998); and W - WUNDER (1998). Identical symbols have been used for the experimental data sets of YA and KA as well as for UT and BN (consistent phase assemblages). The dashed curves show reactions determined by LUTH (1995); the solid curves are compatible with the other experimental studies. Reaction (14), the first occurrence of the 10Å phase with increasing pressure, has been located according to the data of YAMAMOTO and AKIMOTO (1977) and PAWLEY and WOOD (1995). The phase relations about the stability field of E are still uncertain.

shown at high pressures and temperatures on the petrogenetic grid (Fig. 11) are preliminary at best.

A 'petrogenetic grid' for hydrous mantle compositions

The experimental information summarized in the foregoing sections has been used to construct a con-

sistent phase equilibrium diagram for relevant bulk compositions bounded by the phases forsterite - enstatite - H₂O. Figure 9 displays a Schreinemaker's grid approximately oriented in pressure-temperature space. The relevant equilibria are listed in Table 2. Reactions around invariant points IX and X are drawn by thin lines. Invariant point IX involves re-

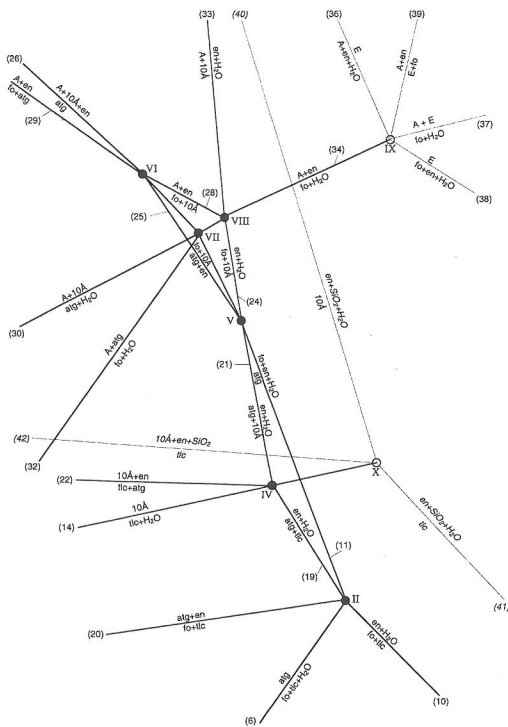


FIG. 9. Schematic pressure-temperature grid for phase relations in the MSH system. Reactions and invariant points are numbered with arabic and roman numbers respectively corresponding to reactions as listed in the text and Table 2. Thick, solid lines refer to MSH equilibria affecting the hydrated mantle bulk composition from Fig. 5. Thin lines refer to other equilibria or highly uncertain (n° 39–42) reactions.

actions producing phase E, which are not well constrained experimentally; the orientation of these reactions in P-T space is ambiguous. Invariant point X includes coesite and is relevant for SiO_2 -saturated compositions not realized in mantle compositions.

The configuration of the invariant points V, VI, VII, and VIII is shown as an enlargement on Fig. 10. Several possible grids for this configuration were tested using the following field and experimental constraints: (1) Reaction $\text{A} + \text{en} = \text{fo} + \text{H}_2\text{O}$ (34) is stable and points away from the triangular region towards high temperature and pressure; (2) Reaction $\text{atg} = \text{fo} + \text{en} + \text{H}_2\text{O}$ (11) is stable and points to lower temperatures; (3) the 10\AA -phase has a stability field in P-T space. The proposed topology was the only one satisfying these constraints and explains well the observed phase assemblages in the experimental studies. An important result of the derived multi-system is the occurrence of the reaction antigorite + H_2O = phase A + 10\AA -phase (30); this reaction does not occur when chrysotile or lizardite

stoichiometries ($\text{Mg}_3\text{Si}_2\text{O}_5(\text{OH})_4$) are used. Instead, a reaction $\text{ctl} = \text{A} + 10\text{\AA} + \text{H}_2\text{O}$ describes the breakdown of the serpentine– H_2O tie-line. The consequence of this change in reaction resulting from the smaller amount of H_2O contained in antigorite than in chrysotile or lizardite is considerable: Conventional experimental methods, i.e. H_2O -saturated conditions, result in the disappearance of antigorite and the formation of the assemblage $10\text{\AA} + \text{A} + \text{H}_2\text{O}$ at considerably lower pressures than the final breakdown of antigorite to phase A + 10\AA -phase + enstatite (26) which is an H_2O -conserving reaction. Thus, it is not possible to study the stability of antigorite on its own stoichiometry in a straightforward way. In nature, the amount of free volatile coexisting with antigorite and forsterite must be very small, because the rock porosity at conditions of more than 5 GPa is negligible, and therefore only very small amounts of phase A + 10\AA phase can form at reaction (30). The stable paragenesis is antigorite + forsterite \pm phase A until forsterite + antigorite react to phase A + enstatite (reaction (29)) at considerably higher pressure. Note, however, that the triangular stability field of the assemblage forsterite + 10\AA -phase collapses if either the H_2O activity becomes reduced or the antigorite stability is increased as observed by BOSE and NAVROTSKY (1998). This leads to stability of the reaction antigorite = phase A + en + H_2O , which is metastable in the presented phase diagram topology (Figs. 9 and 10), but has been proposed by BOSE and GANGULY (1995) and BOSE and NAVROTSKY (1998) to occur in the absence of the 10\AA -phase.

We prefer the derivation of a quantitative phase diagram (Fig. 11) for mantle bulk compositions in the MSH-system from a combination of the experimental phase equilibria constraints (Figs. 6, 7, and 8) with the multi-system analysis (Figs. 9 and 10) over that from a thermodynamic calculation for the following reasons: (1) unresolved differences in the experimental data on antigorite breakdown; (2) uncertainties in the various thermodynamic data bases due to an undefined structural state of antigorite (see also BOSE and NAVROTSKY, 1998); (3) lack of thermodynamic data for the 10\AA -phase and phase E (PAWLEY *et al.*, 1995); (4) lack of an appropriate model for the high pressure volumetric properties of antigorite and H_2O ; and (5) unknown H_2O -activity due to high solubility of MgO and SiO_2 in an H_2O -fluid at high pressure (MANNING, 1994; MIBE *et al.*, 1997).

In Fig. 11, solid lines identify reactions observed in a hydrous mantle composition, whereas thin lines indicate reactions encountered only by compositions outside the range of normal mantle rocks. The following assemblages dominate the pressure-

Table 2. Phase equilibria in the MgO-SiO₂-H₂O system used to construct the P-T grids (Figures. 9 & 10)

Reactions	Reactions
<i>Invariant point II [10Å,A]</i>	<i>Invariant point VII [tlc,en]</i>
(6) atg = 18 fo + 4 tlc + 27 H ₂ O	(23) 5 atg = 90 fo + 20 10Å + 95 H ₂ O
(10) fo + tlc = 5 en + H ₂ O	(27) 24 atg = 85 A + 154 10Å + 14 fo
(11) atg = 14 fo + 20 en + 31 H ₂ O	(30) 45 A + 71 10Å = 11 atg + 7 H ₂ O
(19) atg + 14 tlc = 90 en + 45 H ₂ O	(31) 5 A + 3 10Å = 22 fo + 24 H ₂ O
(20) 45 fo + 31 tlc = atg + 135 en	(32) 3 atg + 20 A = 142 fo + 153 H ₂ O
<i>Invariant point IV [fo,A]</i>	<i>Invariant point VIII [atg,tlc]</i>
(14) 10Å = tlc + 2H ₂ O	(24) fo + 10Å = 5 en + 3 H ₂ O
(19) atg + 14 tlc = 90 en + 45 H ₂ O	(28) 6 fo + 10Å = 8 en + A
(21) atg + 14 10Å = 90 en + 73 H ₂ O	(31) 5 A + 3 10Å = 22 fo + 24 H ₂ O
(22) 73 tlc + 2 atg = 45 en + 180 10Å	(33) A + 5 10Å = 22 en + 18 H ₂ O
<i>Invariant point V [tlc,A]</i>	(34) A + 3 en = 5 fo + 3 H ₂ O
(11) atg = 14 fo + 20 en + 31 H ₂ O	<i>Invariant point IX [10Å,atg,tlc]</i>
(21) atg + 14 10Å = 90 en + 73 H ₂ O	(34) A + 3 en = 5 fo + 3 H ₂ O
(23) 5 atg = 90 fo + 20 10Å + 95 H ₂ O	(36) 100 E = 21 A + 83 en + 57 H ₂ O
(24) fo + 10Å = 5 en + 3 H ₂ O	(37) 4 A + 60 E = 83 fo + 84 H ₂ O
(25) 3 atg + 95 en = 73 fo + 31 10Å	(38) 20 E = 21 fo + 4 en + 24 H ₂ O
<i>Invariant point VI [tlc,H₂O]</i>	(39) 24 A + 84 en = 60 E + 57 fo
(25) 3 atg + 95 en = 73 fo + 31 10Å	<i>Invariant point X [fo,A,atg]</i>
(26) 18 atg = 73 A + 113 10Å + 14 en	(14) 10Å = tlc + 2H ₂ O
(27) 24 atg = 85 A + 154 10Å + 14 fo	(40) 10Å = 3 en + coe + 3 H ₂ O
(28) 6 fo + 10Å = 8 en + A	(41) tlc = 3 en + coe + H ₂ O
(29) 3 atg + 113 fo = 31 A + 154 en	(42) 3 tlc = 10Å + 6 en + 2 coe
<i>Metastable reaction connecting metastable invariant point [tlc,fo] and [tlc,10Å]</i>	
(35) 5 atg = 14 A + 142 en + H ₂ O	

Invariant points II, IV, V, VI, VII, and VIII involve the phases atg, fo, en, tlc, 10Å, A, and H₂O; invariant point IX involves phase E (absence of atg, tlc, 10Å); invariant point X is an extension into the SiO₂ saturated MSH-system (absence of atg, fo, A), not relevant for mantle compositions, but used to delimit the stability of talc and of the 10Å-phase in the MSH system.

temperature diagram: forsterite + talc at low pressures and intermediate to high temperatures, forsterite + antigorite at low temperatures and intermediate to high pressures, phase A + en at high pressures and forsterite + enstatite at high temperatures. Additional small fields with phase assemblages containing phase A and/or the 10Å-phase occur in a rather small P-T interval between 4.0 and 7.5 GPa and at low temperatures of ≤500°C to 620°C.

The transport of H₂O deep into the mantle during subduction of hydrated peridotitic mantle is confined to the forsterite-antigorite starting composition. Only very cold subduction paths, which bypass the critical conditions of 6 GPa and 600°C at the low temperature side, will transport any H₂O beyond this pressure corresponding to a depth of 180 km. Any mantle rock which is subjected to pressure-temperature condition inside the forsterite + enstatite stability field, will completely lose its H₂O stored in hydrous minerals. This conclusion has been drawn by LUTH (1995) based on his experiments on the reaction phase A + enstatite = forsterite + H₂O.

Beyond 200 km the assemblage phase A + enstatite has a very large stability field and will transport a

maximum amount of H₂O of approximately 4.5 wt.% beyond 300 km. The importance of phase E and other DHMS as H₂O-carriers in the mantle transition zone and beyond is discussed in chapter 16 by D. FROST.

HYDRATE MINERALS STABILIZED IN MANTLE COMPOSITIONS BY ADDITIONAL COMPONENTS

The simplified MSH and FMSH (FeO-MgO-SiO₂-H₂O) systems represent approximately 86–96 wt.% of the total oxide components of harzburgitic to lherzolitic mantle and have therefore been the target of most experimental and theoretical studies on the stability of hydrate minerals relevant for the mantle. The remaining 4 to 6 wt.% (excluding FeO) are Al₂O₃, CaO, Cr₂O₃, Na₂O, NiO and TiO₂. Potassium-rich bulk compositions represented by phlogopite and K-richterite bearing peridotites occur only locally and are the product of K-metasomatism not related to the dehydration of subducted peridotitic mantle. Therefore the stability of K-hydrate silicates is not discussed here, but the reader is referred to several recent studies (SUDO and TATSUMI, 1990; LUTH, 1997;

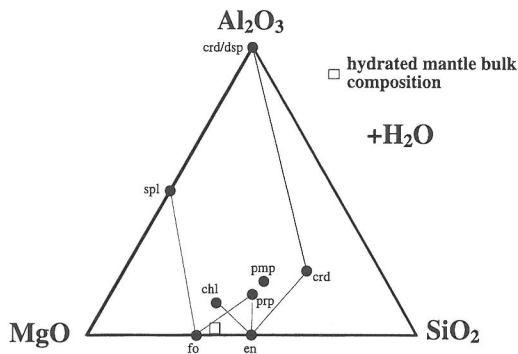


FIG. 12. Projection from H_2O on the plane Al_2O_3 - MgO - SiO_2 . Phases that have been recorded in experiments relevant for the hydrous mantle bulk composition are indicated with abbreviations after KRETZ (1983) and are listed in Table 1.

mal' mantle composition, as long as Ca and Na stabilize plagioclase. At intermediate pressures (0.3 to 2 GPa) spinel + forsterite + enstatite form the breakdown assemblage of clinocllore, and at higher pressures (2 to 5 GPa), the assemblage forsterite + spinel + pyrope-garnet is formed upon dehydration of chlorite. At pressures exceeding 5 to 5.5 GPa, and temperatures below $750^\circ C$ a new hydrate phase is observed in the MASH system (at clinocllore composition), a $MgAlSi$ -hydrate with the pumpellyite structure (Table 1, pmp, SCHREYER and MARESCH, 1991; FOCKENBERG, 1995).

The experimental brackets are consistent among the different experimental studies (Fig. 13), except for the high-pressure brackets of STAUDIGEL and SCHREYER (1977) at 3.5 GPa and that of FOCKENBERG (1995) at 3.3 GPa. The clinocllore stability determined by FOCKENBERG (1995) is 20 – $30^\circ C$ lower than that of STAUDIGEL and SCHREYER (1977), such minor discrepancies are probably within the combined uncertainties in pressure and temperature and variation in the starting materials and run times. Unlike antigorite, which has a composition close to the mantle composition in terms of MgO (+ FeO) and SiO_2 , this is not the case for chlorite. The clinocllore composition, representing the typical chlorite composition found in hydrated harzburgites in high pressure metamorphic terrains, is considerably displaced towards the Al_2O_3 corner of the MAS compositional triangle (Fig. 12) relative to the 'hydrated mantle bulk composition'. Consequently, the absolute stability of chlorite on its own composition may not represent its stability in a mantle-like composition. The mantle bulk composition is located below the tie-line forsterite - pyrope (fo-prp on Fig. 12), therefore only if this tie-line is broken, but the crossing tie-line enstatite + chlorite occurs, can chlorite be present in

a mantle composition. The occurrence of chlorite is therefore delimited by reactions stabilizing the chl + en assemblage. At high pressures and low temperatures, FOCKENBERG (1995) observed the paragenesis forsterite + diasprore + Mg -pumpellyite + H_2O . An inspection of Fig. 12 shows that this assemblage lies above the "hydrated mantle bulk composition", which is located below the fo - pmp tie-line, in a triangle bound by forsterite-enstatite-pyrope or forsterite-enstatite-spinel. Mg -pumpellyite can only occur if pyrope is not stable. FOCKENBERG (1995) has investigated also the stability of pyrope + H_2O , which lies at approximately $100^\circ C$ lower temperature than the maximum stability of Mg -pumpellyite.

A topological analysis of a part of the MASH system (projected from $MgMgAl$ -pumpellyite; not considering quartz/coesite-saturated assemblages) has been performed in order to establish the stable phase assemblages containing chlorite and $MgMgAl$ -pumpellyite for mantle-like compositions (Fig. 14). The exact locations of the enstatite + chlorite reactions shown on Fig. 14 are unknown. The following experimental data infer that they do not differ very

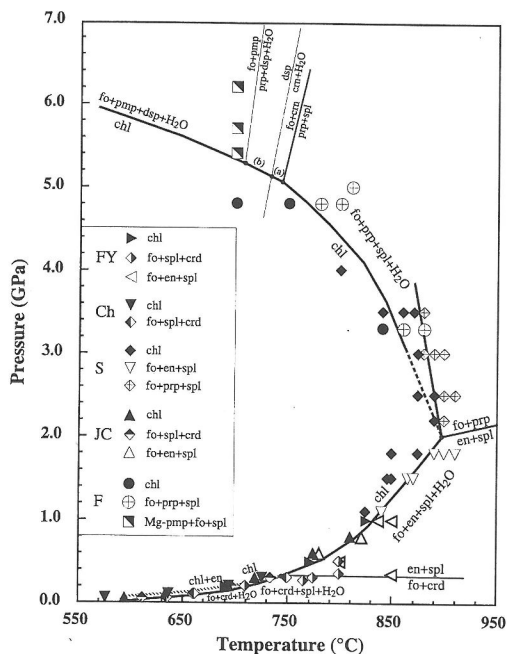


FIG. 13. Experimental data points on chlorite (clinocllore) stability. Mineral abbreviations are listed in Table 1. Experimental fits are eyeball fits of data by FY - FAWCETT and YODER (1966); Ch - CHERNOSKY (1974); S - STAUDIGEL and SCHREYER (1977); JC - JENKINS and CHERNOSKY (86); and F - FOCKENBERG (1995). Reactions (a) and (b) are: chl = fo + prp + crn + H_2O and chl = fo + prp + dsp + H_2O respectively.

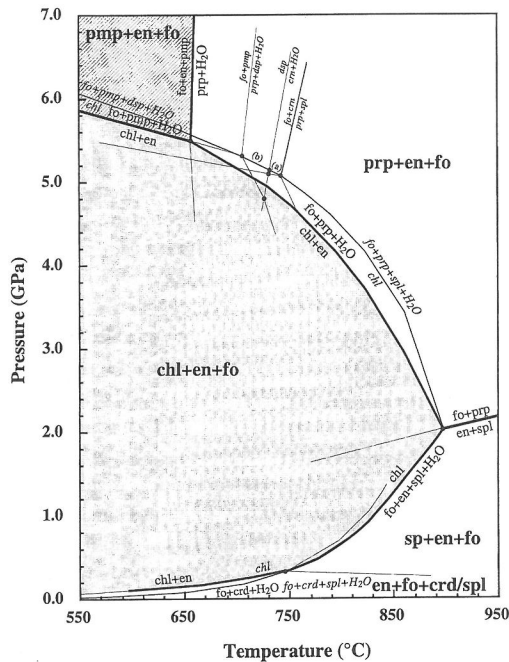


FIG. 14. Pressure-temperature projection for phase relationships in the $\text{H}_2\text{O}-\text{Al}_2\text{O}_3-\text{MgO}-\text{SiO}_2$ system relevant for hydrous mantle bulk compositions. Assemblages that can coexist with an H_2O -fluid and that include the hydrous mantle bulk composition are indicated for the various divariant fields. Mineral abbreviations are listed in Table 1.

much from the absolute stability limits of chlorite: (1) JENKINS and CHERNOSKY (1986) determined the reaction $\text{chl} + \text{en} = \text{fo} + \text{crd} + \text{H}_2\text{O}$ and found an extremely small difference to the chlorite breakdown $\text{chl} = \text{fo} + \text{crd} + \text{spl} + \text{H}_2\text{O}$; (2) FOCKENBERG (1995) reports an experiment at 5.4 GPa/700°C containing the assemblage $\text{chl} + \text{fo} + \text{pmp} + \text{dsp} + \text{en}$ which is close to the final breakdown of chlorite and an experiment at 5.5 GPa/640°C which contains $\text{chl} + \text{en} + \text{pmp}$. Figure 14 shows the stability field for chlorite and Mg-pumpellyite in "hydrous mantle compositions": The stability field of each phase is smaller than the maximum stability on its own stoichiometry. This effect is much smaller for chlorite than for Mg-pumpellyite. The stability condition for the pumpellyite phase is: low temperatures, high pressure and absence of chlorite. Below 5 GPa the temperature difference between the chlorite and antigorite breakdown curves is large (200°C at 2.5 GPa). This implies that in the hotter parts of the slab or in general during slow and therefore hotter subduction, some of the H_2O stored in chlorite survives the antigorite breakdown. Chlorite contains about 20 to 25% of the total H_2O (2 to 2.5 wt.% H_2O) stored in a hydrated Iherzolite to harzburgite composition in

the stability field of forsterite + antigorite + chlorite. The critical conditions of complete dehydration to the anhydrous assemblage pyrope + enstatite + forsterite occurs at 5.6 GPa and 650°C which compares with 6 GPa and 600°C for the MSH system. The stability fields of aluminous phases in upper mantle compositions do not permit transfer of H_2O , liberated by the breakdown of antigorite, into the stability region of DHMS phases.

In conclusion, chlorite is an important H_2O -carrier at intermediate depth (60–150 km), but does not provide the 'vehicle' to transport H_2O deep into the mantle at high pressures and elevated temperatures.

Ti-clinohumite stability in TiO_2 - and F-bearing systems

Titanium- or F-rich clinohumites occur in chlorite, spinel and garnet-peridotites from the Alps, Liguria, Dabie-Shan and other ultramafic massifs (TROMMSDORFF and EVANS, 1980; SCAMBELLURI *et al.*, 1995; ZHANG *et al.*, 1995). Ti-clinohumites are always subordinate. The pure hydroxyl-endmembers of the humite group minerals, such as hydroxyl-clinohumite and chondrodite, are only stable in the MgO-rich part of the MSH system at pressures of less than 4–5 GPa. At higher pressure the forsterite- H_2O tie-line is not present, and Mg-rich phases with Mg/Si ratios > 2 coexist with enstatite. WUNDER *et al.* (1995), PAWLEY and WOOD (1996) and WUNDER (1998) studied the stabilities of humite group minerals and other DHMS phases in the silica-poor part of the MSH system and found large stability fields for Mg-rich DHMS phases.

In the systems containing TiO_2 or F, humite group minerals can coexist with enstatite over a wide pressure range as evidenced by the field occurrences of OH-F Ti-clinohumite. ENGI and LINDSLEY (1980) have studied the stability and breakdown of a Ti-clinohumite, containing the maximum amount of TiO_2 ($x_{\text{Ti}} = 0.5$), to 2.5 GPa. They observed the breakdown of Ti-clinohumite (Ti-chu) to olivine + ilmenite + H_2O . Ti-chu was stable to 600°C at 2.5 GPa. WEISS (1997) extended the range to 8 GPa and studied the influence of variable TiO_2 -contents and F-contents in the system. Natural starting materials were used (avoiding polysomatic intergrowth of synthetic Ti-bearing humite minerals), except for pure F-chu. Figure 15 summarizes the stability fields for clinohumites containing various amounts of TiO_2 , FeO and F. Fluorine stabilizes clinohumite to much higher temperatures (+700°C at 2.5 GPa, Fig. 15). This effect is observed in many hydrates, when F substitutes for OH. Even small amounts of F will have a prominent effect on the stability of clinohu-

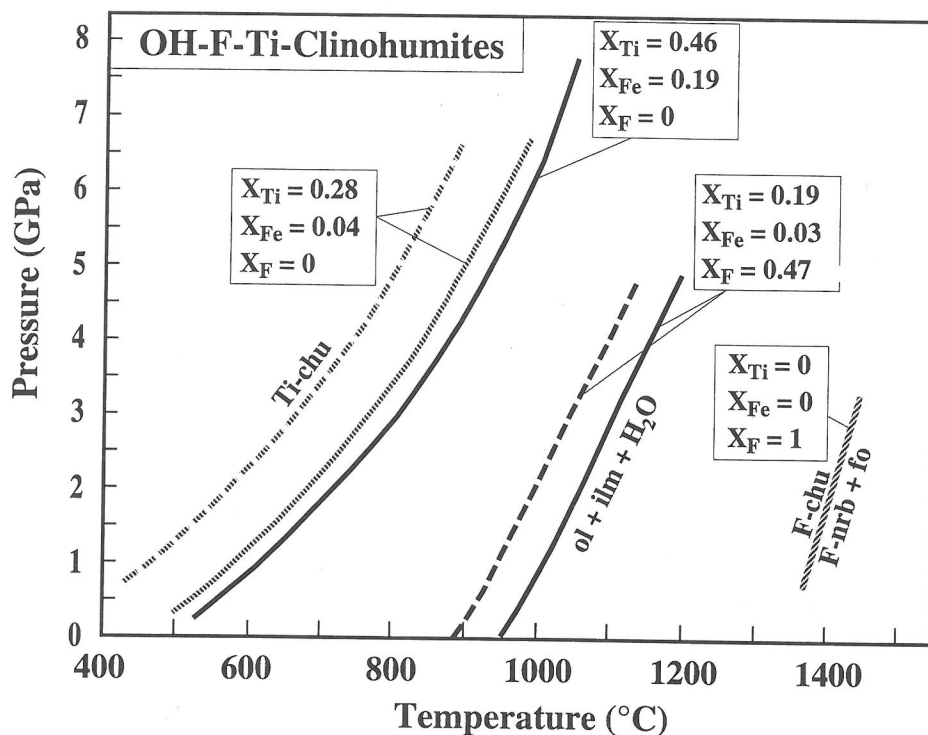


FIG. 15. Experimental curves of the breakdown reactions of natural hydroxyl-titanian clinohumite, of fluorine-hydroxyl-titanian clinohumite, and of synthetic fluorine clinohumite, after WEISS (1997). The divariant fields in which reactants and products coexist are enveloped by dashed and solid lines. Mineral abbreviations are listed in Table 1. The curve label $x_{\text{Ti}} = 0.46$, $x_{\text{Fe}} = 0.19$, $x_{\text{F}} = 0$ refers to the upper stability limit of natural fluorine-free hydroxyl-titanian clinohumite. $X_{\text{Ti}} = \frac{2 \cdot \text{Ti}}{2 \cdot \text{Ti} + \text{OH}}$

mite. Ti-undersaturated OH-chu or F-OH-Ti-bearing clinohumites form divariant reaction bands: Ti- and/or F-undersaturated OH-clinohumites react to olivine + ilmenite + Ti/F-richer clinohumite + H₂O over 60–100°C (Fig. 15). Such divariant reaction bands are also observed in nature (EVANS and TROMSDORFF, 1983): F-rich clinohumite is surrounded by a rim of olivine + ilmenite intergrowth. The pure F-chu reacts to F-norbergite + olivine.

Ti-saturated hydroxyl-clinohumite is the most common clinohumite composition found in ultramafic rocks. At 2 GPa the breakdown of Ti-chu occurs above that of antigorite, and above 3.5 GPa the breakdown occurs above that of chlorite. The quantity of Ti-clinohumite in mantle rocks is small, limited by the TiO₂ content of peridotitic mantle, which does not exceed 0.1 to 0.15 wt%. Even if all this TiO₂ is stored in Ti-clinohumite, its potential as an H₂O-carrier is small, with a maximum amount of H₂O of 1000 to 1500 ppm. The Ti-rich humite phase, however, may significantly control the high field strength element (HFSE) concentrations of fluids emanating from the peridotite during the breakdown of

antigorite or chlorite. Like other Ti-rich phases, Ti-clinohumite strongly concentrates HFSE elements (WEISS, 1997) and thus contributes to the HFSE-depleted characteristic for island-arc magmas generated above subduction zones.

Storage of H₂O in NAMS (nominally anhydrous minerals)

The determinations of the OH-contents of nominally anhydrous minerals, such as olivine, pyroxenes, and garnet (for a review see ROSSMAN, 1996) showed that considerable amount of H₂O (up to several 1000 ppm) can be accommodated in their structure. Experiments by KOHLSTETT *et al.* (1996) revealed that wadsleyite can accommodate up to several wt% of H₂O. SMYTH and KAWAMOTO (1996) identified a new structural type of wadsleyite with high H₂O-content that is stable to very high temperatures. Thus H₂O contained in NAMS may be transported deep into the earth upper mantle and beyond. The combination of hydrous phases at low pressures and temperatures and NAMS at transition zone conditions allows transport

and storage of H₂O within the entire convecting upper mantle.

CONCLUSIONS

The combination of field observations, experimental phase equilibrium studies and thermodynamic calculations demonstrates that only a limited number of hydrous phases are important H₂O-carriers in subducting hydrous mantle. At the initial stage of subduction antigorite is the dominant H₂O-repository, with subordinate chlorite and tremolite. Tremolite, which only constitutes an H₂O-carrier in Ca-rich lherzolitic compositions, reacts to diopside at less than 80 km. Depending on the temperature - pressure path followed by the subducting lithosphere antigorite and chlorite are stable to 150 to 200 km. At 200 km depth and low temperatures of 600–650°C both antigorite and chlorite react to assemblages containing high-pressure hydrate phases (Fig. 11, phase A, 10Å-phase; Fig. 14, Mg-pumpellyite). At greater depth H₂O will be stored in phase A, which has a very large temperature stability field at high pressures. Eventually phase E can transport H₂O into the mantle transition zone. If the critical conditions of 6 GPa and 600°C for antigorite reacting to forsterite + enstatite + H₂O (11) are bypassed at the low temperature side, most H₂O will be conserved by the reactions forming the 10Å-phase. The 10Å-phase is ultimately lost resulting in a release of 2–3 wt.% H₂O. The high-pressure assemblage phase A + en retains approximately 5 wt.% H₂O. If the assemblage forsterite + enstatite + H₂O is directly formed from antigorite, H₂O can only be stored in NAMS.

The coexistence of several hydrous minerals in the peridotitic part of the subducting slab leads to a more or less continuous supply of H₂O to the overlying mantle wedge below 200 km. This is enforced by the breakdown of hydrous minerals in the overlying basaltic and pelitic layers, which dehydrate over a large temperature - pressure interval (SCHMIDT and POLI, 1998). Continuous H₂O-fluxing of the overlying mantle wedge down to at least 200 km (6 GPa) is therefore expected. Partial melting then most probably occurs as the result of melting point depression in the peridotitic mantle due to the influx of H₂O into the hottest part of the wedge (e.g., KUSHIRO, 1987).

Acknowledgments—We would like to thank Jamie Connolly for his help with the thermodynamic calculations and Marcello Mellini for TEM investigations of run products. We are grateful for discussions with Jürgen Konzett, Bernard Evans, Max Schmidt, Stefano Poli, and Werner Schreyer and we thank Dan Frost and Alison Pawley for their constructive and thorough reviews. This work was supported by the Swiss National Science Foundation grant 2000-050454.97/1.

REFERENCES

- ANGEL R. J., CHOPELAS A., and ROSS N.L. (1992) Stability of high-density clinoenstatite at upper-mantle pressures. *Nature* **358**, 322–324.
- ARAI S. (1975) Contact metamorphosed dunite-harzburgite complex in the Chugoku district, western Japan. *Contrib. Mineral. Petrol.* **52**, 1–16.
- BARNICOAT A. and FRY N. (1986) High-pressure metamorphism of the Zermatt-Saas ophiolite zone, Switzerland. *Lithos* **21**, 227–236.
- BAUER J. F. and SCLAR C. B. (1981) The “10Å- phase” in the system MgO - SiO₂ - H₂O. *Amer. Mineral.* **66**, 576–585.
- BERMAN R. G. (1988) Internally consistent thermodynamic data for minerals in the system Na₂O - K₂O - CaO - MgO - FeO - Fe₂O₃ - SiO₂ - TiO₂ - H₂O - CO₂. *J. Petrol.* **29**, 445–522.
- BOILLOT G., GIRARDEAU J., and KORNPROBST J. (1988) Rifting of the Galicia margin: Crustal thinning and emplacement of mantle rocks on the seafloor. *Proc. Ocean Drilling Prog., Sci. Results* **103**, 741–756.
- BOSE K. and GANGULY J. (1995) Quartz-coesite revisited: Reversed experimental determination at 500–1200°C and retrieved thermochemical properties. *Amer. Mineral.* **80**, 231–238.
- BOSE K. and GANGULY J. (1995) Experimental and theoretical studies of the stabilities of talc, antigorite and phase A at high pressures with applications to subduction processes. *Earth Planet. Sci. Lett.* **136**, 109–121.
- BOSE K. and NAVROTSKY A. (1998) Thermochemistry and phase equilibria of hydrous phases in the system MgO-SiO₂-H₂O: Implications for volatile transport to the mantle. *J. Geophys. Res.* **103**, 9713–9719.
- BOWEN N. L. (1928) *The Evolution of Igneous Rocks*. Dover Publications.
- BOWEN N. L. and TUTTLE O. F. (1949) The system MgO - SiO₂ - H₂O. *Bull. Geol. Soc. Amer.* **60**, 439–460.
- BOYD F. R. and ENGLAND J. L. (1960) Apparatus for phase equilibrium measurement of pressures up to 50 kbars and temperatures up to 1750°C. *J. Geophys. Res.* **65**, 741–748.
- CARMICHAEL D. M. (1978) Metamorphic bathozones and bathogrades: A measure of the depth of postmetamorphic uplift and erosion on a regional scale. *Amer. J. Sci.* **278**, 769–797.
- CARUSO L. J. and CHERNOSKY J. V. JR. (1979) The stability of lizardite. *Can. Mineral.* **17**, 757–769.
- CHERNOSKY J. V. JR. (1974) The upper stability of clinocllore at low pressure and the free energy of formation of Mg-cordierite. *Amer. Mineral.* **59**, 496–507.
- CHERNOSKY J. V. JR. (1982) The stability of clinochrysotile. *Can. Mineral.* **20**, 19–27.
- CHERNOSKY J. V. JR., DAY H. W., and CARUSO L. J. (1985) Equilibria in the system MgO-SiO₂-H₂O: experimental determination of the stability of Mg-anthophyllite. *Amer. Mineral.* **70**, 223–236.
- CHERNOSKY J. V. JR., BERMAN R. G., and BRYNDZIA L. T. (1988) Serpentine and chlorite equilibria. In *Hydrous Phyllosilicates Other than Micas*. (ed. S. W. BAILEY), *Rev. Mineralogy* **19**, 295–346.
- COULTON A. J., HARPER D. S., and O'HANLEY D. S. (1995) Oceanic versus emplacement age serpentinisation in the Josephine ophiolite: Implication for the nature of the Moho at intermediate and slow spreading ridges. *J. Geophys. Res.* **100**, 22245–22260.
- DAY H. D. (1972) Geometrical analysis of phase equilibria

- in ternary systems of six phases. *Amer. J. Sci.* **272**, 711–734.
- DAVIES J. H. and STEVENSON D. J. (1992) Physical model of source region of subduction zone volcanics. *J. Geophys. Res.* **97**, 2037–2070.
- DELANY J. M. and HELGESON H. C. (1978) Calculation of the thermodynamic consequences of dehydration in subducting oceanic crust to 100 kb and $>800^{\circ}\text{C}$. *Amer. J. Sci.* **278**, 638–686.
- DIETRICH V. and PETERS T. (1971) Regionale Verteilung der Mg-Phyllosilikate in den Serpentiniten des Oberhalbsteins. *Schweiz. Mineral. Petrol. Mitt.* **51**, 329–348.
- DOMANIK K. J. and HOLLOWAY J. R. (1996) The stability and composition of phengitic muscovite and associated phases from 5.5. to 11 GPa: Implications for deeply subducted sediments. *Geochim. Cosmochim. Acta* **60**, 4133–4150.
- EVANS B. E. and GUGGENHEIM S. (1988) Talc, pyrophyllite and related minerals. In *Hydrous Phyllosilicates Other than Micas* (ed. S. W. BAILEY), *Rev. Mineralogy* **19**, 225–294.
- EVANS B. E. and FROST B. R. (1975) Chrome-spinel in progressive metamorphism - a preliminary analysis. *Geochim. Cosmochim. Acta* **39**, 959–972.
- EVANS B. E. and TROMMSDORFF V. (1970) Regional metamorphism of ultramafic rocks in the Central Alps: parageneses in the system $\text{CaO-MgO-SiO}_2\text{-H}_2\text{O}$. *Schweiz. Mineral. Petrol. Mitt.* **50**, 481–492.
- EVANS B. E. and TROMMSDORFF V. (1983) Fluorine-hydroxyl titanian clinohumite in Alpine recrystallized garnet peridotite: Compositional controls and petrologic significance. *Amer. J. Sci.* **283-A**, 355–369.
- EVANS B. E., JOHANNES W., OTERDOOM H., and TROMMSDORFF V. (1976) Stability of chrysotile and antigorite in the serpentine multisystem. *Schweiz. Mineral. Petrol. Mitt.* **56**, 79–93.
- FAWCETT J. J. and YODER H. S. (1966) Phase relationships of chlorites in the system $\text{MgO-Al}_2\text{O}_3\text{-SiO}_2\text{-H}_2\text{O}$. *Amer. Mineral.* **51**, 353–380.
- FOCKENBERG T. (1995) New experimental results up 100 kbar in the system $\text{MgO-Al}_2\text{O}_3\text{-SiO}_2\text{-H}_2\text{O}$ (MASH): Preliminary stability fields of chlorite, chloritoid, staurolite, $\text{MgMgAl-pumpellyite}$, and pyrope. *Bochumer geol. Geotech. Arb.* **44**, 39–44.
- FROST B. R. (1975) Contact metamorphism of serpentinite, chloritic black wall and rodingite at Paddy-Go-East Pass, Central Cascades, Washington. *J. Petrol.* **16**, 272–312.
- FRUEH-GREEN G. L., PLAS A., and LÉCUYER CH. (1996) Petrologic and stable isotope constraints on hydrothermal alteration and serpentinization of the shallow mantle at Hess Deep (site 895). In *Proc. Ocean Drilling Prog., Sci. Results* (ed. C. MÉVEL *et al.*) **147**, 255–291.
- FURUKAWA Y. (1993) Depth of decoupling plate interface and thermal structure under arcs. *J. Geophys. Res.* **98**, 20005–20013.
- GREEN D. H. (1973) Experimental melting studies on model upper-mantle composition at high pressure under water-saturated and water-undersaturated conditions. *Earth Planet. Sci. Lett.* **19**, 37–53.
- GREEN H. W. and BURNLEY P. C. (1989) A new self-organizing mechanism for deep-focus earthquakes. *Nature* **341**, 733–737.
- GREEN T. H. (1980) Island arc and continent-building magmatism - a review of petrogenetic models based on experimental petrology and geochemistry. *Tectonophysics* **63**, 367–385.
- HONDA S. and UYEDA S. (1983) Thermal process in subduction zones - a review and preliminary approach on the origin of arc volcanism. In *Arc Volcanism: Physics and Tectonics*. (eds. D. SHIMOZURU and I. YOKOYAMA). Terra Scientific Publishing Company.
- ISHI K. and SAITO M. (1973) Synthesis of antigorite. *Amer. Mineral.* **58**, 915–919.
- IRIFUNE T., KUBO N., ISSHIKI M., and YAMASAKI Y. (1998) Phase transformations in serpentine and transportation of water into the lower mantle. *Geophys. Res. Lett.* **25**, 203–206.
- ISHIKAWA T. and NAKAMURA E. (1994) Origin of the slab component in arc lavas from across-arc variation of B and Pb isotopes. *Nature* **362**, 739–743.
- JENKINS D. M. and CHERNOSKY J. V. JR. (1986) Phase equilibria and crystallochemical properties of Mg-chlorite. *Amer. Mineral.* **71**, 924–936.
- JOHANNES W. (1975). Zur Synthese und thermischen Stabilität von Antigorit. *Fort. Mineral. Beihefte* **53**, 36.
- KANZAKI M. (1991) Stability of hydrous magnesium silicates in the mantle transition zone. *Phys. Earth Planet. Inter.* **66**, 307–312.
- KAWAMOTO T., LEINENWEBER K., HERVIG R. L., and HOLLOWAY J. R. (1995) Stability of hydrous minerals in H_2O -saturated KLB-1 peridotite up to 15 GPa. In *Volatiles in the Earth and Solar System* (ed. K. A. FARLEY), pp. 229–239. American Institute of Physics.
- KHODYREV O. Y. and AGOSHKOV V. M. (1986) Phase transitions in the $\text{MgO-SiO}_2\text{-H}_2\text{O}$ system at 40–80 kbar. *Geochem. Int.* **23** (7), 47–52.
- KIRBY S. H., DURHAM W. B., and STERN L. A. (1991) Mantle phase changes and deep-earthquake faulting in subducting lithosphere. *Science* **252**, 216–225.
- KITAHARA S., TAKENOUCI S., and KENNEDY G. C. (1966) Phase relations in the system $\text{MgO-SiO}_2\text{-H}_2\text{O}$ at high temperatures and pressures. *Amer. J. Sci.* **264**, 223–233.
- KOHLSTEDT D. L., KEPPLER H., and RUBIE D. C. (1996) Solubility of water in the alpha, beta and gamma phases of $(\text{Mg,Fe})_2\text{SiO}_4$. *Contrib. Mineral. Petrol.* **123**, 345–357.
- KONZETT J. and ULMER P. (1999) The stability of hydrous potassic phases in lherzolitic mantle - an experimental study to 9.5 GPa in simplified and natural bulk compositions. *J. Petrol.* **40**, 629–652.
- KONZETT J., SWEENEY R. J., THOMPSON A. B., and ULMER P. (1997) Potassium amphibole stability in the upper mantle: an experimental study in a peralkaline KNCMASH system to 8.5 GPa. *J. Petrol.* **38**, 537–568.
- KRETZ R. (1983) Symbols for rock-forming minerals. *Amer. Mineral.* **68**, 277–279.
- KUSHIRO I. (1972) Effect of water on the composition of magmas formed at high pressures. *J. Petrol.* **13**, 311–334.
- KUSHIRO I. (1987) A petrological model of the mantle wedge and lower crust in the Japanese island arcs. In *Magmatic Process: Physicochemical Principles* (ed. B. O. MYSEN), Special Publication No. 1, pp. 165–181. The Geochemical Society.
- KUSHIRO I. (1990) Partial melting of mantle wedge and evolution of island arc crust. *J. Geophys. Res.* **95**, 15929–15939.
- LUTH R. W. (1995) Is phase A relevant to the earth's mantle? *Geochim. Cosmochim. Acta* **59**, 679–682.
- LUTH R. W. (1997) Experimental study of the system phlogopite-diopside from 3.5 to 17 GPa. *Amer. Mineral.* **82**, 1198–1209.
- MANNING C. E. (1994) The solubility of quartz in the lower crust and upper mantle. *Geochim. Cosmochim. Acta* **58**, 4831–4839.

- MASSONE H. J. and SCHREYER W. (1989) Stability field of the high-pressure assemblage talc + phengite and two new phengite barometers. *Eur. J. Mineral.* **1**, 391–410.
- MATTHES S. and KNAUER E. (1981) The phase petrology of the contact metamorphosed serpentinite near Ebendorf, Oberpfalz, Bavaria. *N. Jahrb. Mineral. Abh.* **141**, 59–89.
- MEADE C. and JEANLOZ R. (1991) Deep-focus earthquakes and recycling of water into the Earth's mantle. *Science* **252**, 68–72.
- MELLINI M., TROMMSDORFF V., and COMPAGNONI R. (1987) Antigorite polysomatism: behaviour during progressive metamorphism. *Contrib. Mineral. Petrol.* **97**, 147–155.
- MIBE K., FUJII T., and YASUDA A. (1997) Compositions of aqueous fluid coexisting with mantle minerals at high pressures: The role of water on the differentiation of the mantle. *Terra Nova* **9**, Abstract Supplement **1**, 483 (abstr.).
- MORRIS J. D., LEEMAN W. P., and TERA F. (1990) The subducted component in island arc lavas: constraints from Be isotopes and B-Be systematics. *Nature* **344**, 31–36.
- MYSEN B. O. and BOETTCHER A. L. (1975) Melting of hydrous mantle. I: Phase relations of natural peridotite at high pressure and high temperatures with controlled activities of water, carbon dioxide, and hydrogen. *J. Petrol.* **16**, 520–548.
- MYSEN B. O. and BOETTCHER A. L. (1975) Melting of hydrous mantle. II: Geochemistry of crystals and liquids formed by anatexis of mantle peridotite at high pressures and high temperatures as a function of controlled activities of water, hydrogen, and carbon dioxide. *J. Petrol.* **16**, 549–593.
- MULLER M. R., ROBINSON C. J., MINSHULL T. A., WHITE R. S., and BICKLE M. J. (1997) Thin crust beneath ocean drilling program borehole 735B at the Southwest Indian Ridge. *Earth Planet. Sci. Lett.* **148**, 93–107.
- NAVON O. and STOLPER E. M. (1988) Geochemical consequences of melt percolation: The upper mantle as a chromatographic column. *J. Geol.* **95**, 285–307.
- NIDA K. and GREEN D. H. (1999) Stability and chemical composition of pargasitic amphiboles in MORB pyrolyte under upper mantle conditions. *Contrib. Mineral. Petrol.* **135**, 18–40.
- O'HANLEY D. S. (1991) Fault-controlled phenomena associated with hydration and serpentine recrystallization during serpentinization. *Can. Mineral.* **29**, 21–35.
- O'HANLEY D. S. (1996) *Serpentinities - Records of Tectonic and Petrological History*. Oxford Monographs on Geology and Geophysics. Oxford University Press.
- OTTERDOM W. H. (1978) Tremolite- and diopside-bearing serpentine assemblages in the CaO-MgO-SiO₂-H₂O multicomponent system. *Schweiz. Mineral. Petrol. Mitt.* **58**, 127–138.
- PACOLO R. E. G. and GASPARIK T. (1990) Reversals of the orthoenstatite - clinoenstatite transition at high pressures and high temperatures. *J. Geophys. Res.* **95**, 15853–15858.
- PAWLEY A. R. (1994) The pressure and temperature stability limits of lawsonite; Implications for H₂O recycling in subduction zones. *Contrib. Mineral. Petrol.* **118**, 275–302.
- PAWLEY A. R. (1998) The reaction talc + forsterite = enstatite + H₂O: New experimental results and petrological implications. *Amer. Mineral.* **83**, 51–57.
- PAWLEY A. R. and WOOD B. J. (1995) The high-pressure stability of talc and 10Å phase: Potential storage sites of H₂O in subduction zones. *Amer. Mineral.* **80**, 998–1003.
- PAWLEY A. R. and WOOD B. J. (1997) The low-pressure stability of phase A, Mg₇Si₂O₈(OH)₆. *Contrib. Mineral. Petrol.* **124**, 90–97.
- PAWLEY A. R., REDFERN S. A. T., and WOOD B. J. (1995) Thermal expansivities and compressibilities of hydrous phases in the system MgO-SiO₂-H₂O: talc, phase A and 10Å-phase. *Contrib. Mineral. Petrol.* **122**, 301–307.
- PEACOCK S. M. (1990) Numerical simulations of metamorphic pressure-temperature-time paths and fluid production in subducting slabs. *Tectonics* **9**, 1197–1211.
- PISTORIUS C. W. F. T. (1963) Some phase relations in the system MgO-SiO₂-H₂O to high pressures and temperatures. *N. Jahrb. Mineral., Monatshefte* **11**, 283–293.
- PLANK T. and LANGMUIR C. H. (1993) Tracing trace elements from sediment input to volcanic output at subduction zones. *Nature* **362**, 739–743.
- POLI S. and SCHMIDT M. W. (1995) Water transport and release in subduction zones: experimental constraints on basaltic and andesitic systems. *J. Geophys. Res.* **100**, 22299–22314.
- RALEIGH C. B. and PATERSON M. S. (1965) Experimental deformation of serpentinite and its tectonic implications. *J. Geophys. Res.* **70**, 3965–3985.
- RINGWOOD A. E. (1974) The petrological evolution of island arc systems. *J. Geol. Soc. Lond.* **130**, 183–204.
- RINGWOOD A. E. and MAJOR A. (1967) High-pressure reconnaissance investigation in the system Mg₂SiO₄-MgO-H₂O. *Earth Planet. Sci. Lett.* **2**, 130–133.
- ROSSMAN G. R. (1996) Studies of OH in nominally anhydrous minerals. *Phys. Chem. Mineral.* **23**, 299–304.
- SANFORD R. F. (1981) Mineralogical and chemical effects of hydration reactions and applications to serpentinization. *Amer. Mineral.* **66**, 290–297.
- SCAMBELLURI M., MUENTENER O., HERMANN J., PICCARDO G. B., and TROMMSDORFF V. (1995) Subduction of water into the mantle: History of an alpine peridotite. *Geology* **23**, 459–462.
- SCHMIDT M. W. (1996) Experimental constraints on recycling of potassium from subducted oceanic crust. *Science* **272**, 1927–1930.
- SCHMIDT M. W. and POLI S. (1994) The stability of lawsonite and zoisite at high pressures: Experiments in CASH to 92 kbar and implications for the presence of hydrous phases in subducted lithosphere. *Earth Planet. Sci. Lett.* **124**, 105–118.
- SCHMIDT M. W. and POLI S. (1998) What causes the position of the volcanic front? Experimentally based water budget for dehydrating slabs and consequences for arc magma generation. *Earth Planet. Sci. Lett.* **163**, 361–379.
- SCHNEIDER M. E. and EGGLEER D. H. (1986) Fluids in equilibrium with peridotite minerals: Implications for mantle metasomatism. *Geochim. Cosmochim. Acta* **50**, 711–724.
- SCHREYER W., MARESC W. V., and BALLER T. (1991) A new hydrous, high-pressure phase with a pumpellyite structure in the system MgO-Al₂O₃-SiO₂-H₂O. In *Progress in Experimental Petrology* (ed. L. L. PERCHUK), pp. 47–64. Cambridge University Press.
- SILVER P. G., BECK S. L., WALLACE T. C., MEADE C., MYERS S., JAMES E., and KUEHNEL R. (1995) Rupture characteristics of the deep Bolivian earthquake of June 9 1994 and the mechanism of deep-focus earthquakes. *Science* **268**, 69–73.
- SMYTH J. R. and KAWAMOTO T. (1997) Wadsleyite II; a new high pressure hydrous phase in the peridotite-H₂O system. *Earth Planet. Sci. Lett.* **146**, 9–16.
- SPRINGER R. K. (1974) Contact metamorphosed ultramafic rocks in the western Sierra Nevada foothills, California. *J. Petrol.* **15**, 160–195.

- STAUDIGEL H. and SCHREYER W. (1977) The upper thermal stability of clinocllore, $Mg_3Al[AlSi]_3O_{10}(OH)_8$, at 10–35 kb P_{H_2O} . *Contrib. Mineral. Petrol.* **61**, 187–198.
- STOLPER E. and NEWMAN S. (1994) The role of water in the petrogenesis of Mariana trough magmas. *Earth Planet. Sci. Lett.* **121**, 293–325.
- SUDO A. and TATSUMI Y. (1990) Phlogopite and K-amphibole in the upper mantle: Implications for magma genesis in subduction zones. *Geophys. Res. Lett.* **17**, 29–32.
- TATSUMI Y. (1986) Origin of subduction zone magmas based on experimental petrology. In *Physics and Chemistry of Magmas* (eds. L. PERCHUK and I. KUSHIRO), pp. 268–301. Springer.
- TATSUMI Y., SAKUYAMA M., FUKUYAMA H., and KUSHIRO I. (1983) Generation of arc basalt magmas and thermal structure of the mantle wedge in subduction zones. *J. Geophys. Res.* **88**, 5815–5825.
- TATSUMI Y. and NAKAMURA N. (1986) Composition of aqueous fluid from serpentinite in the subducted lithosphere. *Geochem. J.* **20**, 191–196.
- TATSUMI Y., HAMILTON D. L., and NESBITT R. W. (1986) Chemical characteristics of fluid phase released from a subducted lithosphere and origin of arc magmas: Evidence from high pressure experiments and natural rocks. *J. Volcanol. Geotherm. Res.* **29**, 293–309.
- THOMPSON A. B. (1992) Water in the Earth's upper mantle. *Nature* **358**, 295–302.
- TROMMSDORFF V. (1983) Metamorphose magnesiumreicher Gesteine: Kritischer Vergleich von Natur, Experiment und thermodynamischer Datenbasis. *Fort. Mineral.* **61**, 283–308.
- TROMMSDORFF V. and EVANS B. W. (1972) Progressive metamorphism of antigorite schist in the Bergell Tonalite Aureole (Italy). *Amer. J. Sci.* **272**, 423–437.
- TROMMSDORFF V. and EVANS B. W. (1974) Alpine metamorphism of peridotitic rocks. *Schweiz. Mineral. Petrol. Mitt.* **54**, 333–352.
- TROMMSDORFF V. and EVANS B. W. (1980) Titanium hydroxyl clinohumite: Formation and breakdown in antigorite rocks (Malenco, Italy). *Contrib. Mineral. Petrol.* **72**, 229–242.
- TROMMSDORFF V., LOPEZ SANCHEZ-VIZCAINO V., GOMEZ-PUGNAIRE M. T., and MÜNTENER O. (1998) High pressure breakdown of antigorite to spinifex-textured olivine and orthopyroxene, SE Spain. *Contrib. Mineral. Petrol.* **132**, 139–148.
- UEHARA S. and SHIROZU H. (1985) Variations in chemical composition and structural properties of antigorite. *Mineral. J. (Japan)* **12**, 299–318.
- ÜLMER P. and TROMMSDORFF V. (1995) Serpentine stability to mantle depths and subduction-related magmatism. *Science* **268**, 858–861.
- WEISS M. (1997) Clinohumites: A field and experimental study. Ph.D. dissertation 12202, Swiss Federal Institute of Technology (ETH), Zurich, 168p.
- WUNDER B. (1998) Equilibrium experiments in the system $MgO-SiO_2-H_2O$ (MSH): stability fields of clinohumite-OH [$Mg_9Si_4O_{16}(OH)_2$], chondrodite-OH [$Mg_5Si_2O_8(OH)_2$] and phase A [$Mg_7Si_2O_8(OH)_6$]. *Contrib. Mineral. Petrol.* **132**, 111–120.
- WUNDER B. and SCHREYER W. (1997) Antigorite: High-pressure stability in the system $MgO-SiO_2-H_2O$ (MSH). *Lithos* **41**, 213–227.
- WUNDER B., BARONNET A., and SCHREYER W. (1997) Ab-initio synthesis and TEM confirmation of antigorite in the system $MgO-SiO_2-H_2O$. *Amer. Mineral.* **82**, 760–764.
- WUNDER B., PODLESSKII K. K., and SCHREYER W. (1995) Phase relations of Dense Hydrous Magnesium Silicates up to 100 kbar. *Bochumer Geol. Geotech. Arb.* **44**, 269–274.
- WYLLIE P. J. (1971) Role of water in magma generation and initiation of diapiric uprise in the mantle. *J. Geophys. Res.* **76** 1328–1338.
- YAMAMOTO K. and AKIMOTO S.-I. (1977) The system $MgO-SiO_2-H_2O$ at high pressures and temperatures - stability field for hydroxyl-chondrodite, hydroxyl-clinohumite and 10Å-phase. *Amer. J. Sci.* **277**, 288–312.
- YODER H. S. (1952) The $MgO-Al_2O_3-SiO_2-H_2O$ system and the related metamorphic facies. *Amer. J. Sci. Bowen Volume*, 569–627.
- ZHANG R. Y., LIU J. G., and CONG B. L. (1995) Talc-, magnesite-, and Ti-clinohumite-bearing ultrahigh-pressure meta-mafic and ultramafic complex in the Dabie Mountains, China. *J. Petrol.* **36**, 1011–1037.

